

AD-A067 430

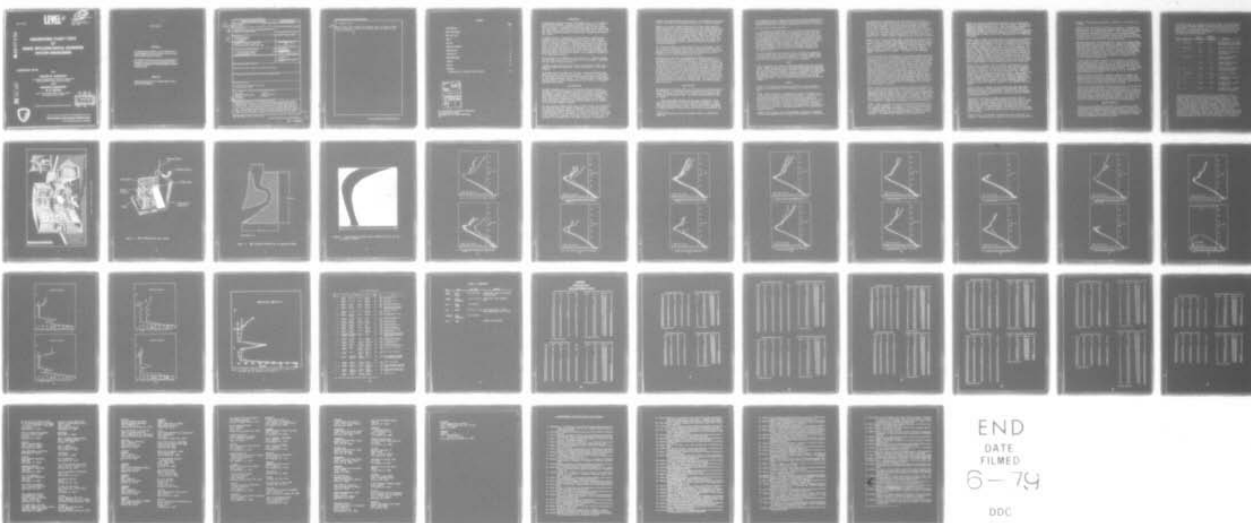
ARMY ELECTRONICS RESEARCH AND DEVELOPMENT COMMAND WS--ETC F/G 4/2
ENGINEERING FLIGHT TESTS OF RANGE METEOROLOGICAL SOUNDING SYSTE--ETC(U)
FEB 79 B W KENNEDY, A KINGHORN, B R HIXON

UNCLASSIFIED

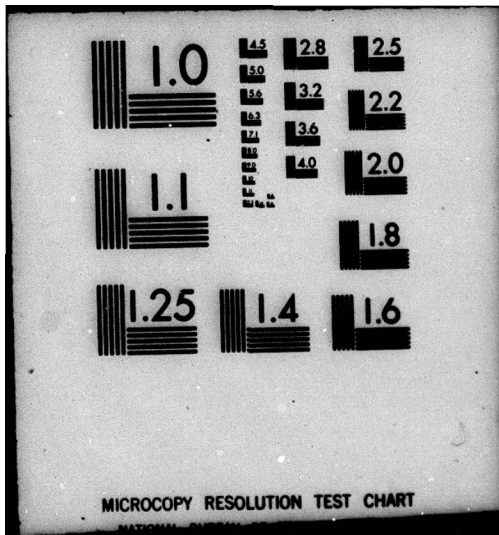
ERADCOM/ASL-TR-0022

NL

1 OF 1
OF 400



END
DATE
FILMED
6-79
DDC



MICROCOPY RESOLUTION TEST CHART

ASL-TR-0022

LEVEL II

AD
Reports Control Symbol
OSD - 1366

AAO 67430

**ENGINEERING FLIGHT TESTS
OF
RANGE METEOROLOGICAL SOUNDING
SYSTEM RADIOSONDE**

FEBRUARY 1979

By

BRUCE W. KENNEDY

**U.S. ARMY ATMOSPHERIC SCIENCES LABORATORY
White Sands Missile Range, New Mexico 88002**

and

ARTHUR KINGHORN

B. R. HIXON

**U.S. NAVY PACIFIC MISSILE TEST CENTER
Point Mugu, California 93043**

DDC FILE COPY

Approved for public release; distribution unlimited

DDC
RECEIVED
APR 19 1979
REGULATED
D



US Army Electronics Research and Development Command

Atmospheric Sciences Laboratory

White Sands Missile Range, NM 88002

9 03 26 159

NOTICES

Disclaimers

The findings in this report are not to be construed as an official Department of the Army position, unless so designated by other authorized documents.

The citation of trade names and names of manufacturers in this report is not to be construed as official Government indorsement or approval of commercial products or services referenced herein.

Disposition

Destroy this report when it is no longer needed. Do not return it to the originator.

20. ABSTRACT (Cont)

cont. and solar shielding are added to the package, results are improved. Operational problems were encountered with the RMSS sonde, and design deficiencies were discovered.



CONTENTS

	<u>Page</u>
INTRODUCTION	2
RMSS RADIOSONDE	2
KMR TEST PLAN	3
TESTS	4
RESULTS	4
RELATIVE HUMIDITY	7
OBSERVATIONS	9
CONCLUSIONS	10
RECOMMENDATIONS	10
FIGURES	11
TABLES	28
APPENDIX	
TABULATED DATA, KWAJALEIN MISSILE RANGE	30

ADDRESS: 97 88	
178	White Center <input checked="" type="checkbox"/>
178	Red Center <input type="checkbox"/>
SPONSORED	<input type="checkbox"/>
JUSTIFICATION	
BY _____	
DISTRIBUTION/AVAILABILITY GROUP	
Dist.	AVAIL. num/yr FORM
A	

RE: ASL-TR-0022, Classified references,
distribution unlimited-
No change per Ms. Marie Richardson,
ASL

INTRODUCTION

The Range Meteorological Sounding System (RMSS) (fig. 1) is an advanced tracking device designed to measure atmospheric parameters to a high degree of accuracy to meet high priority major range and test facility user requirements. Conceived by the Range Commanders Council Meteorological Group, the project was funded by the Navy, Army, and Air Force. The Navy Pacific Missile Test Center assumed project management and contractual control.

The RMSS consists of a ground-based tracking pedestal, automatic data processing computer, 403 MHz ranging transmitter, 1680 MHz telemetry receiver, and a newly developed radiosonde. During a typical mission a sonde is activated, attached to a meteorological balloon, released, and tracked by the ground station. A 403 MHz ranging signal is transmitted back to the ground station along with telemetry data on 1680 MHz. The sonde can monitor four sensors with a rapid, solid-state commutator and typically measure temperature and humidity in the standard configuration. Additional sensors can be added to measure other atmospheric parameters or for comparative purposes.

Data from sensors are displayed in near real-time on a graphics cathode ray tube (CRT), and are listed in tabular form on a printer. Postflight reduction also produces data plots.

The RMSS can also passively track National Weather Service (NWS) radiosondes and PWN8B/11A rocketsondes. Data are recorded on a strip chart recorder.

Acceptance tests of the RMSS were performed at Kwajalein Missile Range (KMR) during the period 16-27 January 1978. At that time the RMSS sonde was also flown in various research and development (R&D) configurations to test sensors and airflow ducts. This report describes the R&D flights, discusses results, makes recommendations on future sondes, and suggests additional test flights.

RMSS RADIOSONDE

The RMSS radiosonde (fig. 2) is a four-channel instrument capable of measuring any selected atmospheric parameter with electrical resistance transducers. In the standard configuration it contains a boom-mounted 10-mil bead thermistor and a duct mounted carbon element hygistor. Two spare channels are available for additional sensors such as pressure, ozone, and hygistor temperature, or standard sensors can be connected to the additional channels, thereby increasing sampling rate. Commutation rate is four frames per second.

The sonde receives ranging pulses with a 403 MHz receiver, and retransmits the range data along with telemetry information on a 1680 MHz downlink. All electronic components except the 1680 MHz transmitter are mounted on a single printed circuit (PC) board. The sonde is approximately 25.4 cm³, weighs 900 grams, and is constructed of closed-cell styrofoam. The hygistor is mounded in an integral airflow duct, while the bead thermistor is attached to an outrigger boom. The 10-mil thermistor is soldered to a

silvered and aluminized mylar loop identical to the PWN8B Loki rocketsonde sensor. The bead is also aluminized to reduce solar radiation heating.

Typically, the sonde is bench tested with an external power supply to adjust ranging and telemetry frequencies and to test sensor performance. Overall sonde and ground station performance is also checked; then a water activated battery replaces the external power supply, the hygistor element is mounted in the duct, and the cover is installed. Sensor performance is again observed on the graphic display. Three nylon cords are wrapped around the styrofoam container to secure the cover, and a four-cord rigging harness is attached. The activated sonde is carried to an elevated platform where baseline computer functions are performed and range bias determined.

The sonde is attached to a meteorological balloon and released. Tracking is automatic during the entire flight, and near real-time data can be observed on both graphics display and in tabulated form. The CRT also displays a plot of relative sensor value as a function of altitude, a convenient way to detect abnormal sensor function.

An integral air duct (fig. 3) which houses the humidity element is a miniaturized version of the NWS NEXAIR duct.* Flow characteristics of the RMSS humidity ducts were made by Messrs M. Krumins and E. Fisher in the US Naval Academy wind tunnel. The results gave rise to hopes of measuring ambient air temperature in the duct near the humidity sensor; thus protecting the fragile 10-mil bead thermistor from damage. Improvements in flow and a decrease in turbulence were detected when the entrance orifice was tilted at a negative 35-degree angle in the wind tunnel. This prompted new design models, and one particular configuration, referred to as Krumins C3 (fig. 4), was found to have excellent flow pattern and very low turbulence in the duct. Reproductions of the C3 duct were made and were included in the R&D test program at KMR. The conclusion was that improved flow would benefit both temperature and humidity measurement in the duct.

KMR TEST PLAN

Representatives of the Army, Navy, and Air Force met in Phoenix, Arizona, in December 1977, and devised a plan to perform R&D tests on the RMSS sonde. At KMR the tests would be in conjunction with acceptance tests of the RMSS during January 1978. The overall sonde problem was stated as follows:

"The current RMSS radiosonde has two major deficiencies. First, the temperature sensor, a 10-mil bead thermistor attached to a loop mount on an extended boom, is very fragile and susceptible to breakage from mishandling and severe weather. Second, the air duct containing the humidity element is known to have poor airflow characteristics and

*Personal discussions with Bruce Bollermann, Space Data Corporation, Tempe, AZ.

is susceptible to solar radiation [electrical] and battery heating effects. It is highly desirable to eliminate the boom and loop mount by moving a thermistor inside the duct providing temperatures are proved to be equal."

The test approach read as follows:

"A minimum of ten RMSS sondes will be required to make engineering changes and perform flight tests. The changes will be minor, and most of them will be done on site at KMR. Space Data Corporation will provide the existing sonde with the following changes: the hygistor mount will be modified to place it in the best airflow location and to isolate it from battery and printed circuit board heat. Opaque material will be placed around the duct walls (outside) to shield the interior sensors from solar radiation. Waxed cardboard or similar material will be placed in the battery cavity to prevent acid damage. Suitable drain holes will be drilled in the styrofoam case to permit drainage of excess battery water."

The basic configuration was changed on site to measure heat conduction to the hygistor, detect flow and turbulence in the duct, measure solar influence, and determine hygistor temperature. Survival tests, particularly in rain, were planned, but nature did not cooperate.

TESTS

Table 1 summarizes the standard and R&D sonde flights that were conducted at KMR. Twenty-two balloon ascents with RMSS radiosondes were made, most with a conjunctive NWS radiosonde. Fourteen of the ascents were dedicated R&D tests, and eight were standard releases. Occasionally, an extra sensor was placed on a standard flight for comparative purposes. The standard configurations were flown for the purpose of acceptance tests on the complete RMSS system. Table 2 lists the sensors used during the R&D test flights.

RESULTS

Flight 0 was a standard configuration released for initial checkout purposes. Timing problems in the incoming line prevented retrieval of data.

Flight 1 (fig. 5) was also a standard sonde, except the hygistor contained a bead thermistor for temperature measurement. Agreement between air temperature, as measured by the loop mount, and the hygistor thermistor was within 4°C up to 14 km, then diverged significantly to a 28°C difference at 35 km. Increases in relative humidity (RH) up to 40 percent were detected above 10 km, but it is not known how meaningful the values are. Therefore, inaccuracies in temperature of the hygistor with respect to air are not considered significant in the computation of relative humidity.

Flights 2 and 3 (figs. 6 and 7) were designed to measure the difference in duct wall temperature with and without cork insulation. In addition,

air temperature was measured with the loop mount on its boom, duct temperature with a post-mounted 10-mil bead thermistor. A second duct was attached side saddle to the sonde and also contained a 10-mil post-mounted bead thermistor. Cork (6 mm thick in two plies) was glued to the battery compartment wall between the battery and duct. Results were positive. The cork decreased duct wall temperature by 9°C at 25 km, but only a 2°C improvement was seen in the duct temperature at 25 km. The added duct, however, measured temperatures that were cooler than the standard duct. Neither, however, compared favorably with the loop mount.

Flight 4 (fig. 8) was a standard sonde, except that the angle of attack of the duct was -35 degrees. This angle was determined by Krumins and Fisher in wind tunnel tests which improved the flow through the standard duct. The temperature difference between the hygistor thermistor and the loop mount at 25 km was 21°C, as opposed to 13°C on flight 1. The change in angle of attack, in fact, degraded the airflow, allowing thermal contamination of the sensor. The reason will be discussed later.

To further evaluate the standard duct for measuring atmospheric temperature, a sonde was flown at -35 degrees angle of attack, and 10-mil bead thermistors were placed in the duct inlet and at the optimum flow region in the duct throat. An additional standard duct attached to the sonde also contained a 10-mil bead in the throat region. Solar shielding was used on the attached duct. Flight 5 (fig. 9) shows the results of this test. The important discovery here was that all sensors in the ducts exhibited large oscillatory excursions above 20 km. There was also significant divergence of the standard duct inlet and throat thermistors from the loop mount above 20 km. Even though the add-on duct appeared to agree more favorably with the loop mount, personal observation of the graphics display revealed unacceptable temperature excursions. Figure 9 is plotted at 1-km intervals, which causes aliasing and is the reason for the apparent better agreement. Close scrutiny of the 1 km data showed a warm-side bias of 2.4°C between 20 to 22.5 km and 2.8°C between 27 to 30 km.

Flight 6 (fig. 10) was an abortive attempt to evaluate the Krumins C3 duct. Sonde problems caused channel dropouts during the flight, so the test was repeated in flight 8 (fig. 11). Channel 2, the C3 duct inlet temperature, went bad before launch. Channel 3, an add-on standard duct with 10-mil bead, and channel 4, the C3 duct containing a 10-mil bead, were flown at angles of -35 and -45 degrees, respectively. The results were conclusive: neither the standard duct nor the Krumins model accurately measured air temperature. Divergence was severe above 20 km.

Flight 7 (fig. 12) tested the ability of the standard duct and the C3 duct to measure humidity. As a point of interest, the temperature of each humidity element was also measured. The standard duct was flown at 0 degrees angle, while the C3 version was at -45 degrees. Between the surface and 5 km, the two hygistors measured virtually the same humidity. A conjunctive NWS radiosonde showed comparable data.

Between 5 to 10 km, the differences were greater than 4 percent; and above 10 km, differences were on the order of 8 percent. The hygistor thermistors offered another picture. There was excellent agreement in temperature between the surface and 25 km, and the standard duct temperature diverged to the warmer side. At 32 km the C3 duct hygistor temperature was 6°C colder than the standard duct hygistor temperature. This difference, however, was of little significance in the measurement of humidity.

Flights 9 and 10 (figs. 13 and 14) offered an examination of a different type of sensor, a 55-mil bead thermistor. The beads were mounted to metal standoff posts similar to the 10-mil thermistors used in previous R&D flights and were attached to a boom which protruded from the side of the sonde. Flight 9 was in daylight, and 10 was in darkness. Each bead was coated with white enamel paint to reduce solar radiation influence. Flight 9 showed a definite divergence between loop mount and 55-mil bead sensors, with the 55-mil bead yielding warmer temperatures above 20 km. This difference was caused primarily by solar radiation. Flight 10, however, showed divergence in the opposite direction, with the 55-mil thermistor reading colder above 20 km. Most of the difference was attributable to lag and radiation cooling, and the two flights give an understanding of solar radiation and lag in the 55-mil bead.

Flight 11 was a diagnostic test to determine the temperature of the commutator during flight. Several previous sondes had been plagued with loss of channels in the vicinity of the tropopause. Temperature influence was suspected, but this flight showed that the commutator temperature varied between only about 20° and 25°C. Later consultation among factory representatives at KMR and in Phoenix revealed that battery condensation probably caused short circuits on the PC board. It was suggested that an overcoat of silicon grease be swabbed on the PC board. This technique proved to be very successful, and later sondes, starting with flight 15, subjected to the procedure were successful.

Flight 12 (fig. 15) compared the loop-mounted bead thermistor with a post-mounted bead. Both were located on the same boom. The post-mounted bead measured air temperature to within 2°C of the loop bead throughout the flight, suggesting that a bias error existed, probably in the calibration data.

Flight 13 (fig. 16) was an attempt to evaluate several types of thermistors. All sensors were boom mounted and coated white for solar reflectivity. The loop bead was aluminized as in all previous tests. Again, sonde electronic problems were encountered (the silicon fix technique had not yet been postulated), but results were still obtained. Channel 2, a 75-mil thermistor was warmer than the loop bead by 8°C at 28 km. An NWS wafer sensor was 9°C warmer, and a 55-mil bead was 6°C warmer.

Flight 14 (fig. 17) contained a standard duct and a C3 duct on 5 cm standoffs. The purpose was to isolate the ducts from the sonde with an

airspace. Results were inconclusive. Channels 2, 3, and 4 quit at 20 to 21 km.

Flight 17 (fig. 18) was the last R&D test in January. A standard duct was mounted on 5 cm standoffs and contained 10-mil beads in the throat and the inlet. The loop-mounted bead was flown on its boom, and an NWS rod thermistor was mounted on the sonde by its outrigger framework. The balloon burst at 19.2 km; however, temperatures started to diverge at about 13 km. Both duct thermistors and the rod read warmer at 16 km, and maintained the differences at balloon burst point.

Additional R&D tests of the RMSS sonde were conducted on 6 April 1978. The first flight (fig. 19) was designed to compare a loop-mounted 10-mil bead thermistor, a post-mounted 10-mil bead thermistor, and an NWS rod thermistor on a standard sonde. Unfortunately, the wrong calibration data were introduced into the computer for channel 2, the post mount, which resulted in erroneous data. During this flight the loop-mounted bead and the rod temperature agreed between the surface and 2 km altitude; then the two sets of data diverged to a constant 3°C with the rod thermistor reading warmer.

Flight 20 was an attempt to compare relative humidity as measured in the standard duct and a standoff duct. The RMSS sonde was placed beside an NWS radiosonde on the same balloon train, and there was radio frequency interference between the two even though the NWS sonde transmitted at 1690 MHz and the RMSS sonde was at 1662 MHz. The interference was detected only on the RMSS ground equipment, not on the AN/GMD-1 (GMD) tracking the NWS sonde.

Flight 21 (fig. 20) compared a hygistor mounted in a standoff duct with one mounted in an NWS duct that was strapped to the RMSS sonde. Temperature of both hygistors was measured. Even though the balloon burst at 13 km, all pertinent data had been collected. Temperature and relative humidity were nearly identical at all levels.

Flight 22 (fig. 21) compared a loop mount, post mount, and rod thermistors during a nighttime release. There appeared to be a 2- to 3-degree bias between the loop- and post-mounted thermistors, a condition that prevailed throughout the flight. This condition is attributed to calibration error. A bias also existed between the loop and the rod, but the magnitude slowly diminished with altitude. Initially, a 6°C difference existed, with the rod reading warmer; but near burst, near 38 km, the bias was only 2°C, again with the rod reading warmer.

RELATIVE HUMIDITY

Flights 2 and 3 measured the difference in wall temperature between the standard duct without and with cork insulation. As would be expected, the cork reduced the wall temperature varying from 2°C at 1 km altitude to 14°C at 10 km. There was also a significant difference in duct air temperature between the two flights which would, of course, affect the computation of relative humidity.

To find out which duct configurations were the best for humidity measurements, RMSS sondes were compared to the nearest NWS conjunctive rawinsonde release. Differences were taken at 1 km levels up to 13 km or the upper limit of the rawinsonde humidity data. The differences were then averaged and standard deviations computed. The following chart shows the comparison (neglecting signs).

Order	Flight No.	Mean Difference	Standard Deviation	Remarks
1	7 (ch 1)	0.38	6.3	Standard duct, with cork and cardboard solar shield
2	21 (ch 3)	1.0	8.9	J005 duct on RMSS sonde
3	9	1.15	6.15	Standard duct with cork and cardboard
4	21 (ch 1)	1.3	9.1	Standoff standard duct with cardboard
5	1	1.85	2.12	Standard duct without cork, cardboard
6	10	-3.25	7.37	Standard duct, without cork, night flight
7	7 (ch 3)	8.6	15.15	C3 duct at -45 deg
8	19	-8.62	8.79	Standard duct, no cork or cardboard
9	12	14.46	3.95	Standard duct, no cork or shielding
10	4	18.46	4.9	Standard duct, -35 deg, no cork or shielding

One could conclude that the addition of cork insulation and solar shielding effectively improved the measurement of humidity. However, flight 1 (fig. 22) was flown without these modifications and still yielded results that were comparable with the NWS rawinsonde. This occurrence can probably be attributed to the tightness of fit between the styrofoam duct and the battery compartment. These parts were hand-cut, and hand-assembled. Therefore, there were slight differences in fit among the sondes that were flown. Perhaps the sonde used on flight 1 fitted snugly and sealed the air leaks between the battery case and air duct. Conversely, flight 4 (fig. 23) shows a large disagreement between the standard sonde and the NWS rawinsonde. In this test, cork and shielding were not used, but the duct was tilted at -35 degrees.

Figures 24 through 29 show additional comparisons between humidity as measured by various RMSS sonde configurations and the NWS rawinsonde. In most cases, the NWS sonde was released within minutes of the RMSS, thereby reducing time and space variability problems. Flights 19 and 21 (figs. 28 and 29) were exceptions. Flight 19 was released 3 hours after the NWS sonde (both were morning flights), while flight 21 was flown 2 hours after a conjunctive rawinsonde (both were afternoon releases). Some variability can be attributed to time and space separation.

Flight 21 was of particular significance because it measured humidity with elements contained in both an RMSS duct mounted on insulating standoffs and in an NWS duct mounted to the side of the RMSS package. The standoff duct was completely covered with opaque cardboard to prevent solar radiation from penetrating through the styrofoam into the duct. As figure 29 shows, the two humidity profiles are nearly identical. Even though this is a sample of one, it adds credibility to the performance of the RMSS standard duct design.

OBSERVATIONS

In this discussion of test results a few words are appropriate about factors that influence performance. Even though wind tunnel tests showed improved flow at different angles of attack and in optimum configurations, the real world is not a tunnel. During one flight, a Super Radot, a precise optical tracker at KMR, recorded over an hour of balloon ascent. The train, which included the sonde and a 12.7 cm aluminum sphere, oscillated like a pendulum. The path of the swing appeared to be elliptical with a period of 6.5 seconds per cycle. In addition, the sonde spun about the string axis giving a very complicated flow pattern throughout the flight. The swing obviously caused the oscillatory temperature on flight 5 and others, and probably contributed to the overall failure to accurately measure air temperature in the duct.

The human engineering aspect is also an important factor. The sonde assembly procedure was tedious and time-consuming. Battery assembly required removal of part of the standard duct assembly. The battery was in the electronics compartment and the moist acid effluent caused PC board malfunctions. The boom on which the loop mount was placed did not have an adequate support and had to be taped for added strength. In short, not much thought was given to the operational requirements for prelaunch preparation and handling. Future designs must diligently pursue this aspect of sonde utility.

The NWS J005 radiosonde was flown in conjunction with most of the KMR test flights, and plots are shown in this report for comparative purposes. The J005 suffered from slow commutation rate and tended to lose some amplitude resolution. Temperature was in good agreement. Above 20 km studies by Ballard and Rubio* show that both solar radiation and lag

*H. N. Ballard and R. Rubio, "Corrections to Observed Rocketsonde and Balloonsonde Temperatures," Journal of Applied Meteorology, October 1968.

conditions exist with the rod. Why then should the rod agree with the 10-mil bead? A probable cause is the inaccuracy of the pressure sensor in the NWS sonde. Pressure altitude errors of up to 5 km have been measured which will cause a misassignment of the temperature versus altitude, and hence an apparent temperature difference. Perhaps the problem is more difficult than that.

Tests 19 and 22 indicate that, except for biases, daytime comparisons between rod and bead are favorable, while at nighttime there are significant differences. On flight 19, a daylight flight, the average temperature difference between the bead and rod (b-r) is -2.1°C below 20 km, and -2.3°C above 20 km. Flight 22, a nighttime release, shows -4.8°C difference below 20 km and -2.7°C above. The primary differences are the solar radiation and the nighttime long wave radiation.

CONCLUSIONS

Three main points concerning the RMSS radiosonde can be made as a result of these test flights. First, air temperature cannot be accurately measured in either the standard duct or the Krumins C3 duct at different angles of attack, or on standoffs. Second, humidity can be measured in the standard duct, with insulation, with solar shielding, and comparable with but more frequently than NWS sondes. Temperature measurement of the hygistor should be continued until total error budget can be determined. Third, the loop-mount bead thermistor measures air temperature more accurately and more frequently than the NWS rod thermistor. However, it appears that the more expensive loop can be replaced with the less expensive post-mounted 10-mil bead thermistor

RECOMMENDATIONS

Extensive RMSS radiosonde flight tests should be conducted to determine optimum sonde housing configuration, sensors to be used and their placement, optimum sensor sampling rate and smoothing techniques, and accuracies of the measurements.

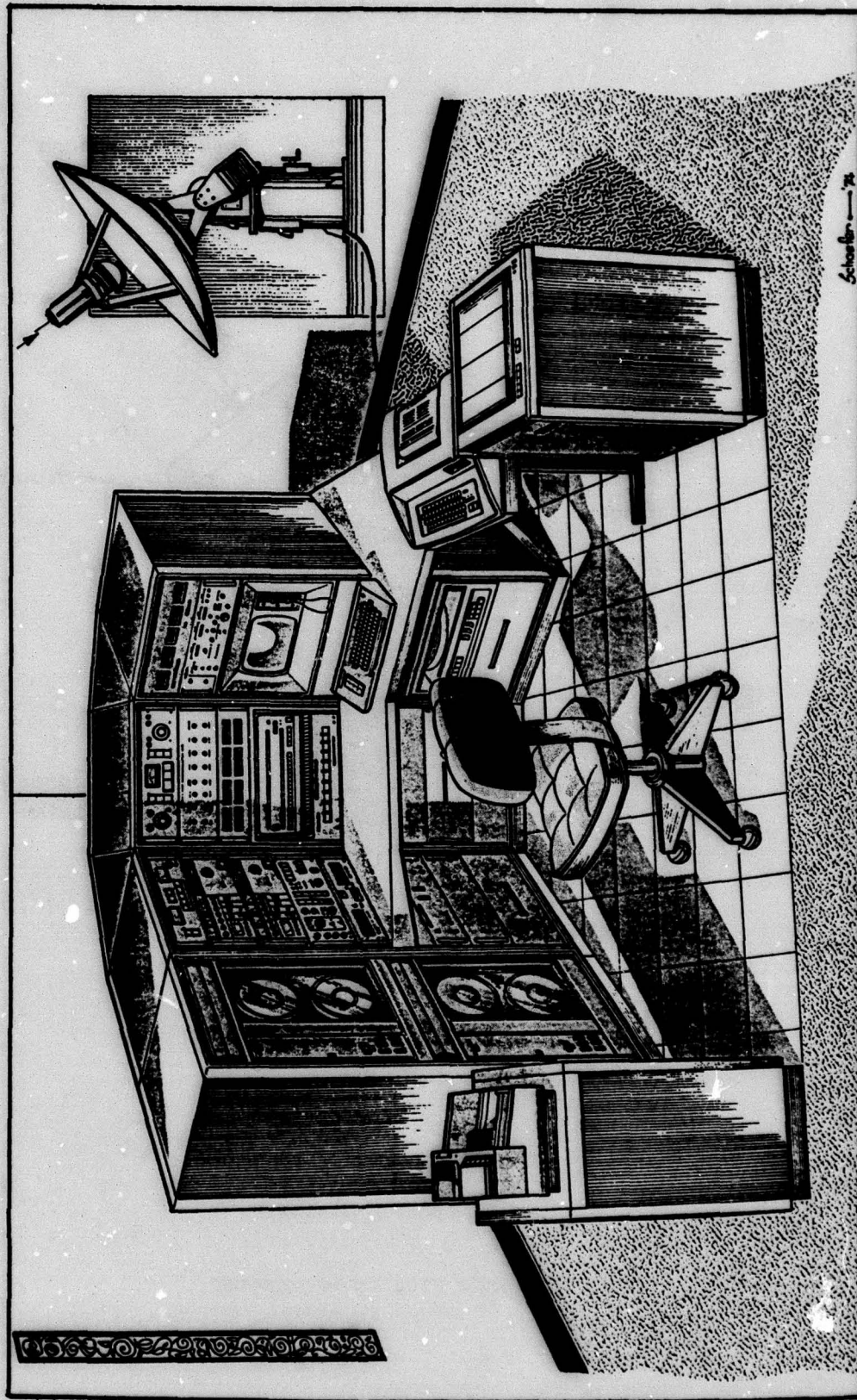


Figure 1. RMSS control console and tracker.

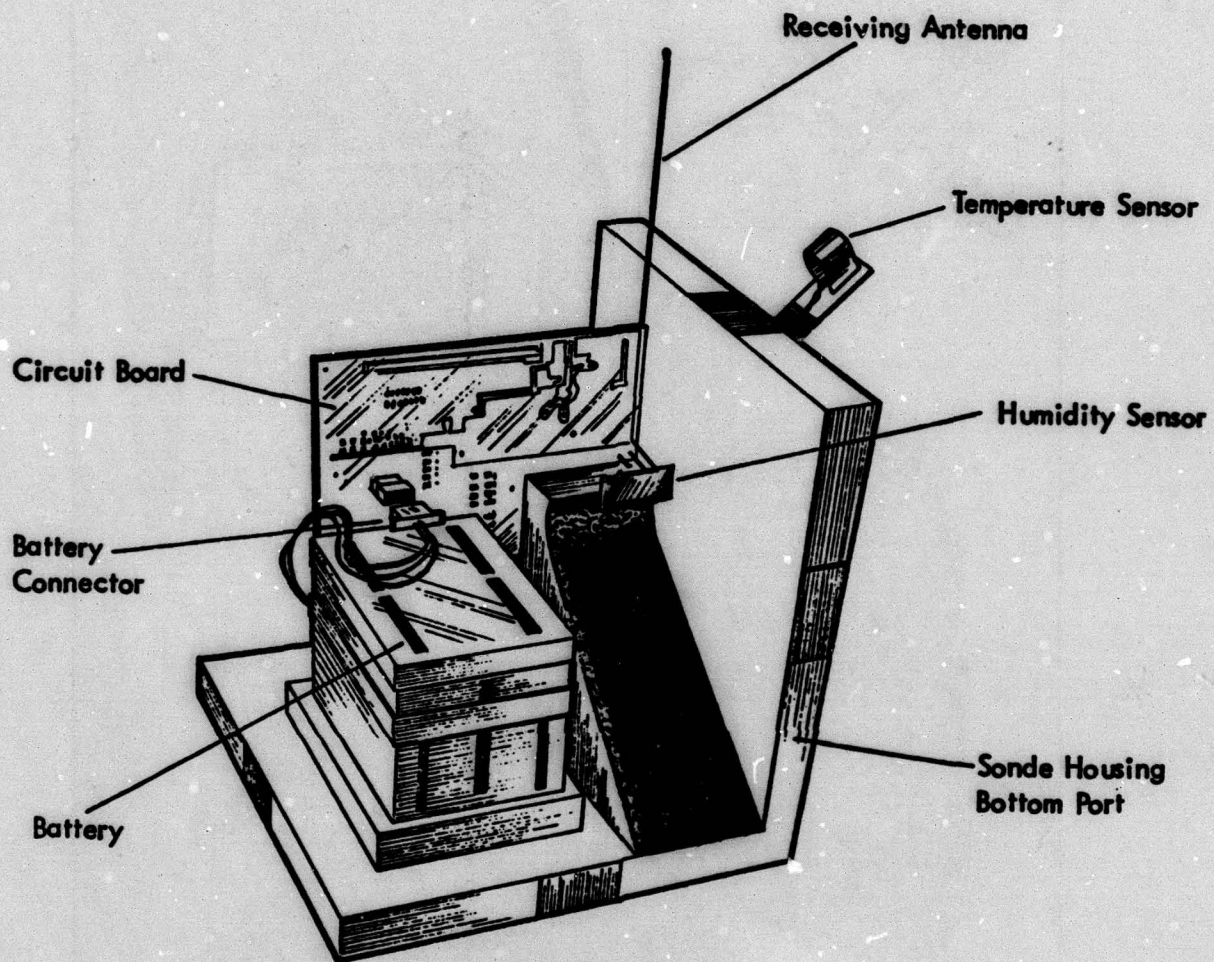
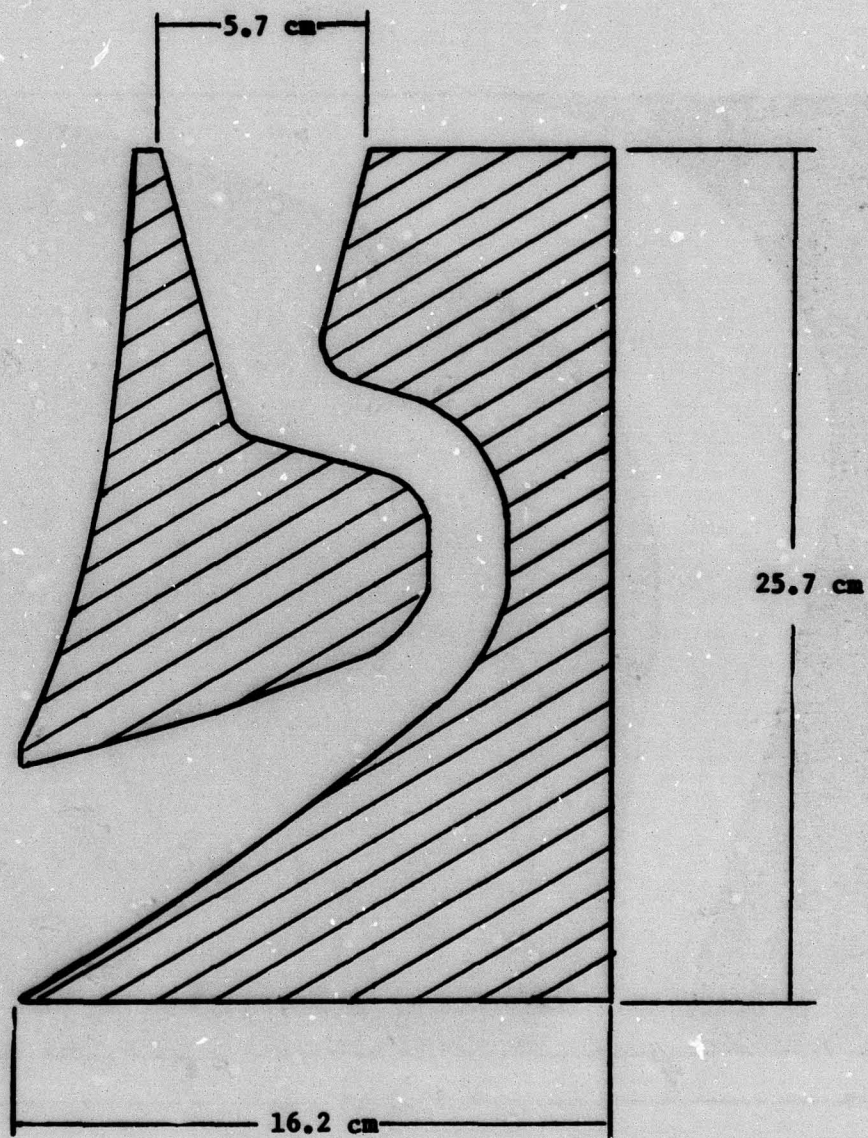


Figure 2. RMS radiosonde with cover removed.



DUCT WIDTH 7 cm

Figure 3. RMSS radiosonde standard duct for hygistor element.

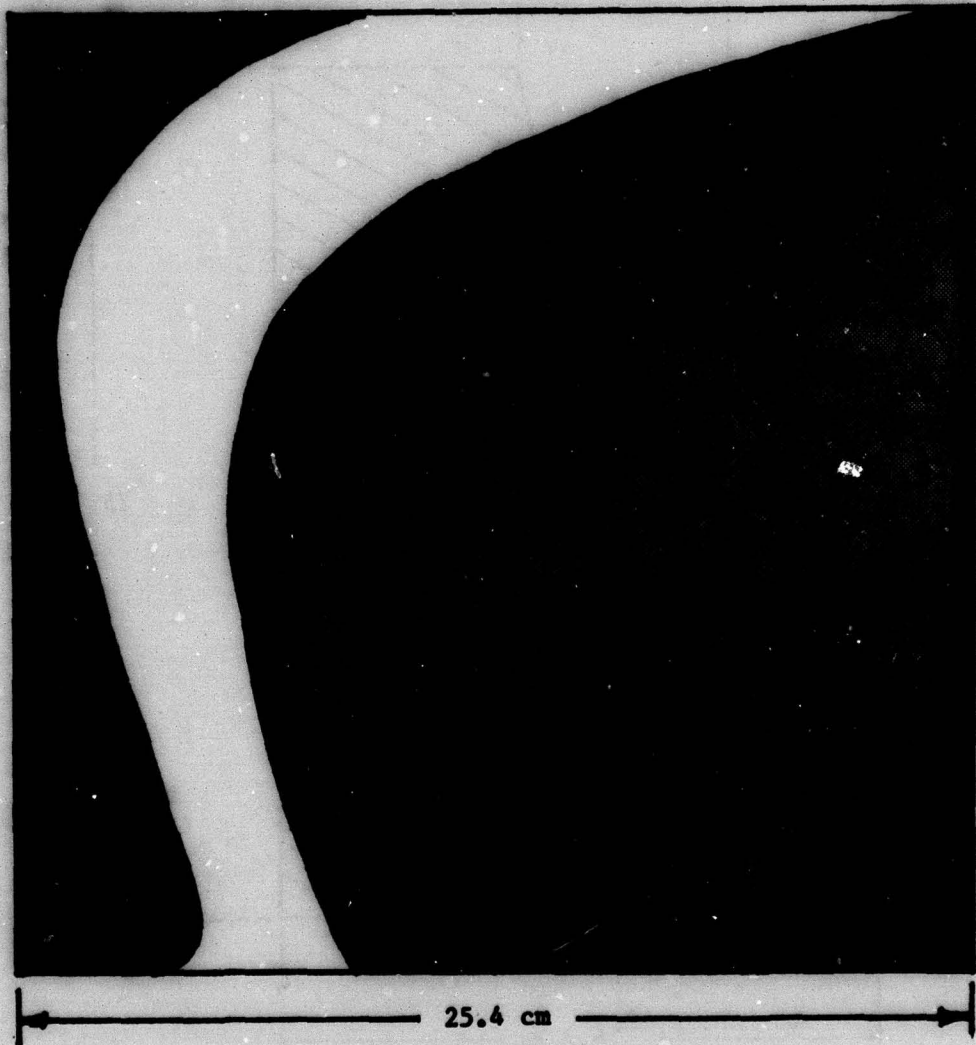


Figure 4. Cross section of Krumins-Fisher configuration three (C3) duct for hygristor element.

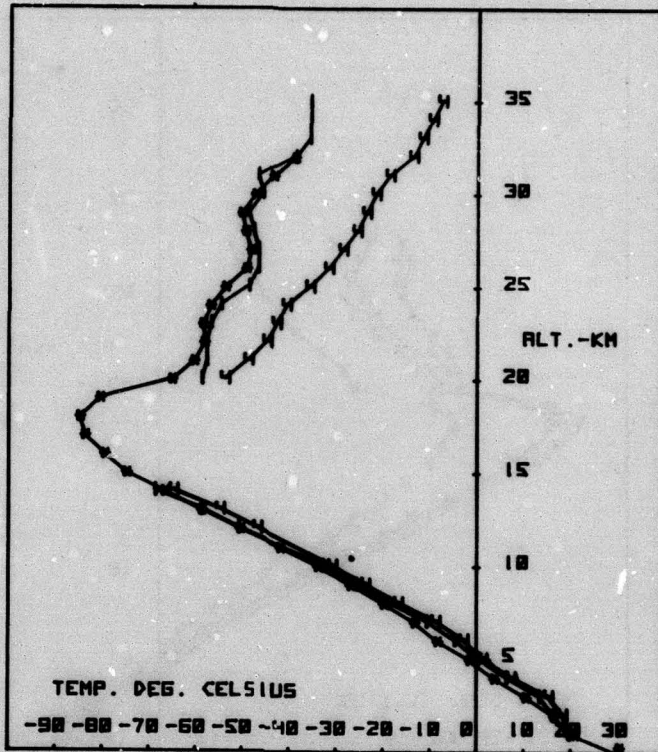


Figure 5. Flight 1; 1-loop mount; 4-hygristor thermistor; *—WWS rawinsonde.

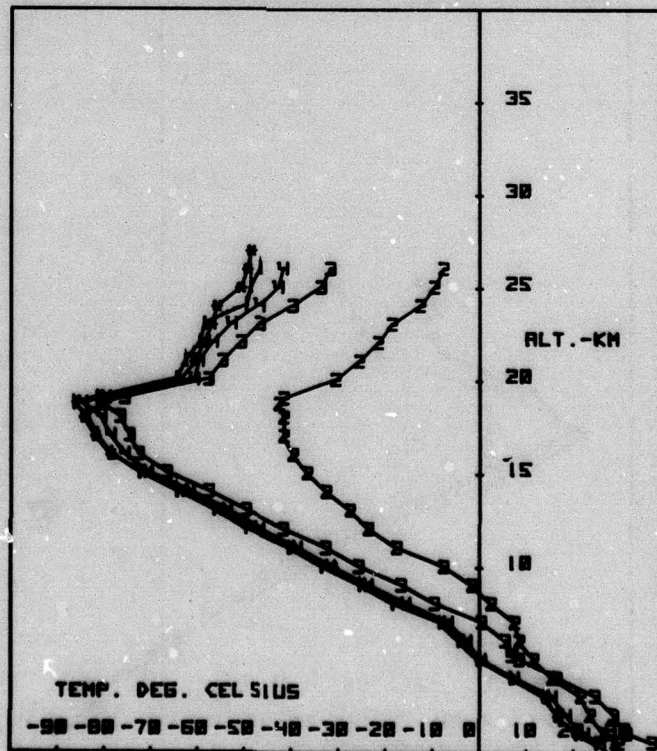


Figure 6. Flight 2; 1-loop mount; 2-standard duct wall temperature; 3-standard duct air temperature; 4-add-on standard duct air temperature; *—WWS rawinsonde.

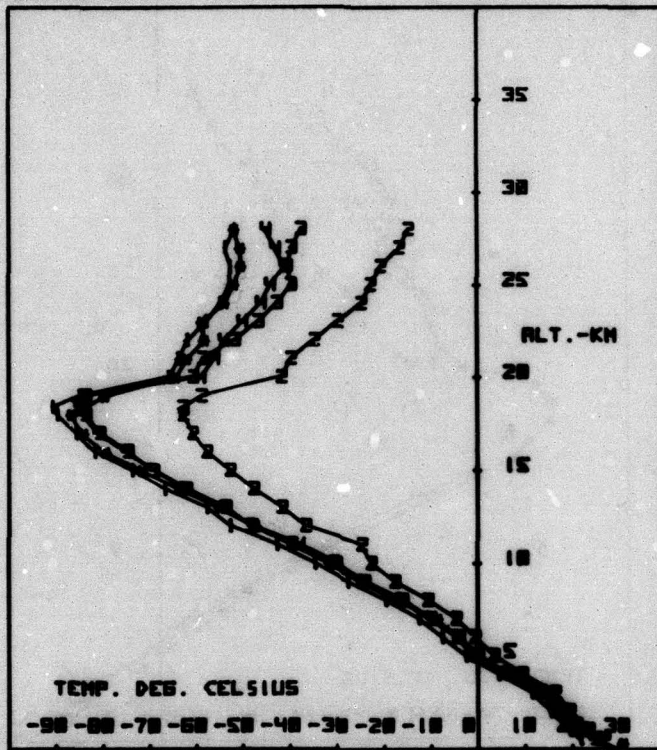


Figure 7. Flight 3; 1-loop mount; 2-standard dust wall temperature; 3-standard dust air temperature; 4-add-on standard dust air temperature; *—DMS rawinsonde.

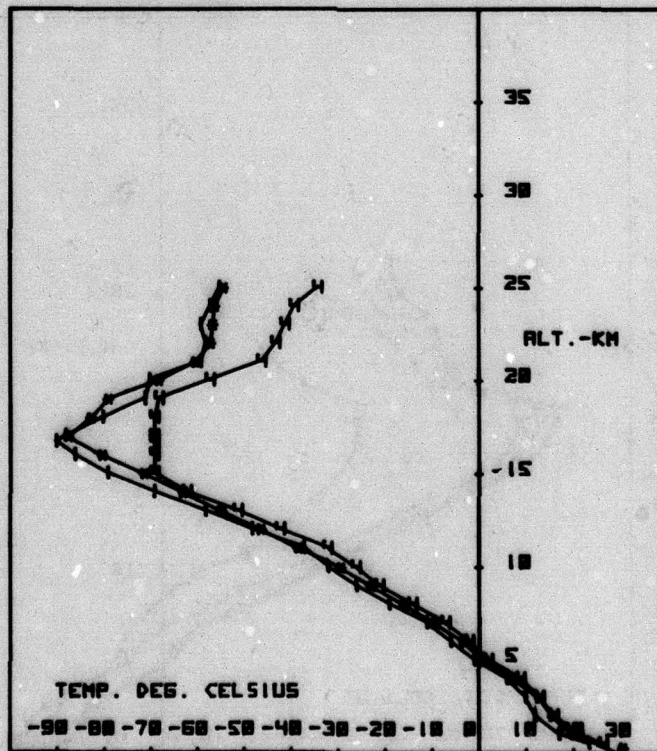


Figure 8. Flight 4; 1-loop mount; 4-hygristor thermometer; *—DMS rawinsonde.

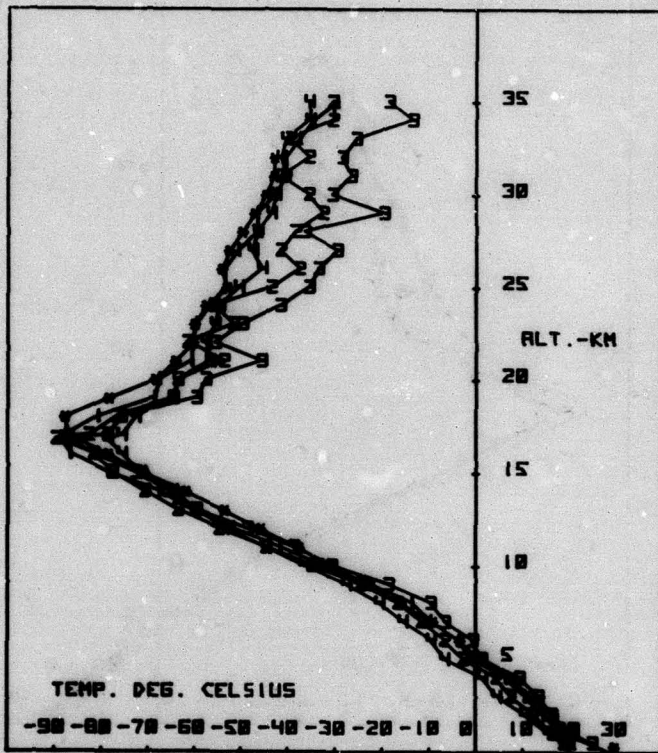


Figure 9. Flight 5; 1-loop mount; 2-thermistor at standard duct entrance; 3-standard duct air temperature; 4-add-on standard duct air temperature; 5-NWS rawinsonde.

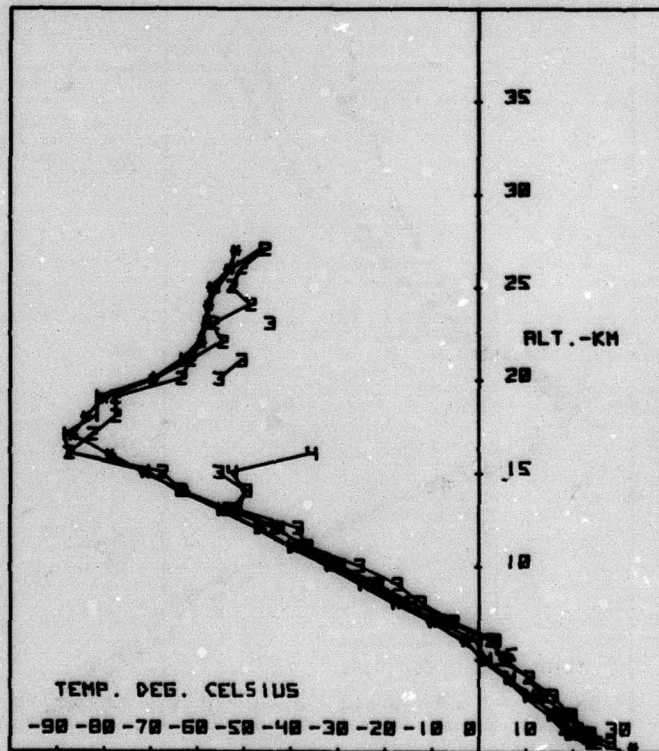


Figure 10. Flight 6; 1-loop mount; 2-C3 inlet thermistor; 3-standard duct air temperature; 4-C3 duct air temperature; 5-NWS rawinsonde.

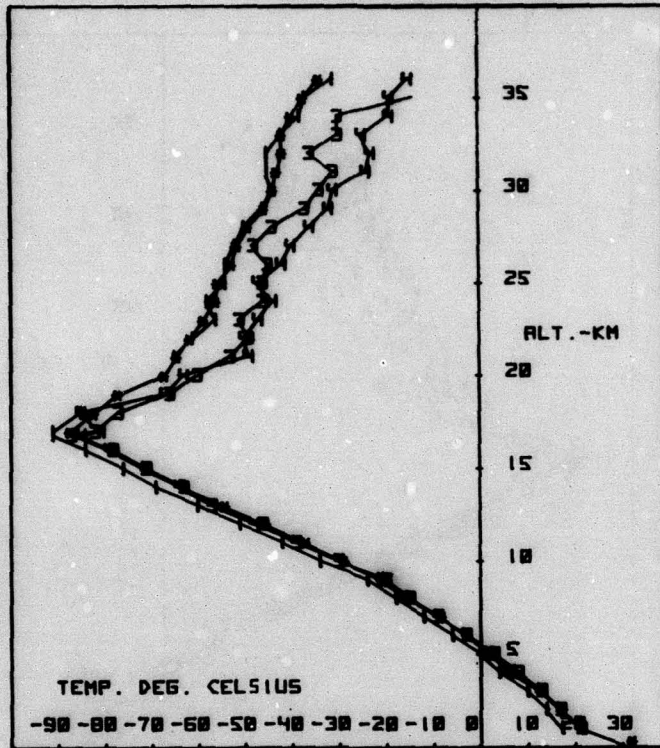


Figure 11. Flight 8; 1-loop mount; 2-C3 inlet thermistor; 3-standard duct air temperature; 4-C3 duct air temperature; \circ -MHS rawinsonde.

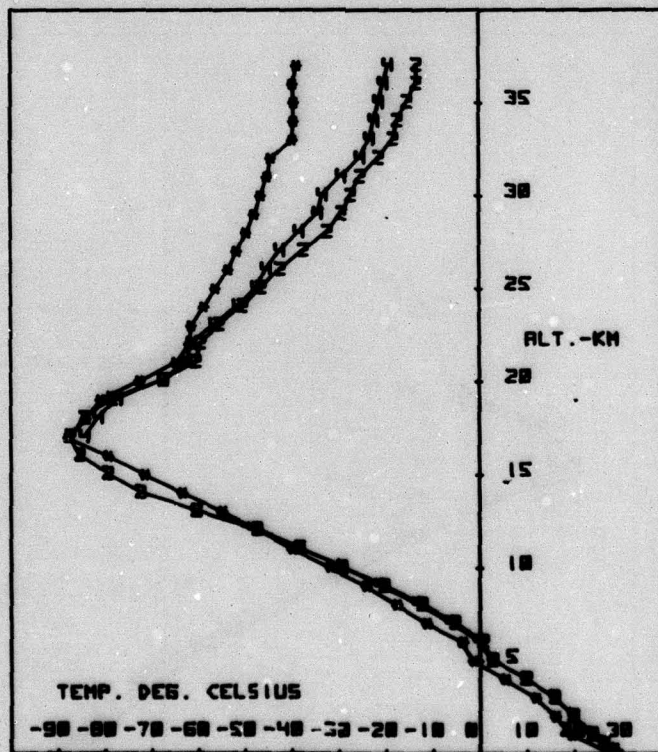


Figure 12. Flight 7; 2-hygristor thermistor in standard duct; 4-hygristor thermistor in C3 duct; \circ -MHS rawinsonde.

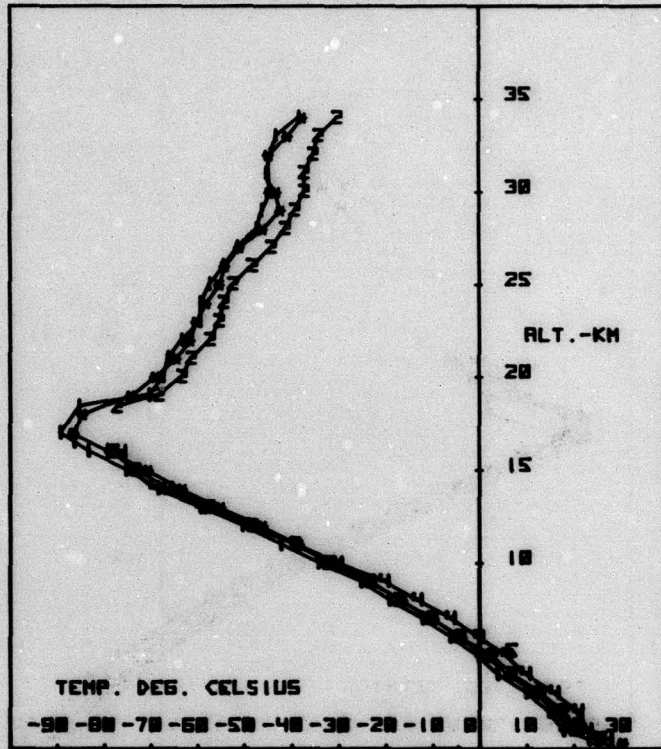


Figure 13. Flight 9; 1-loop mount; 2-TSI thermistor on boom; 4-hygristor thermistor; 6-SWS ramsonde.

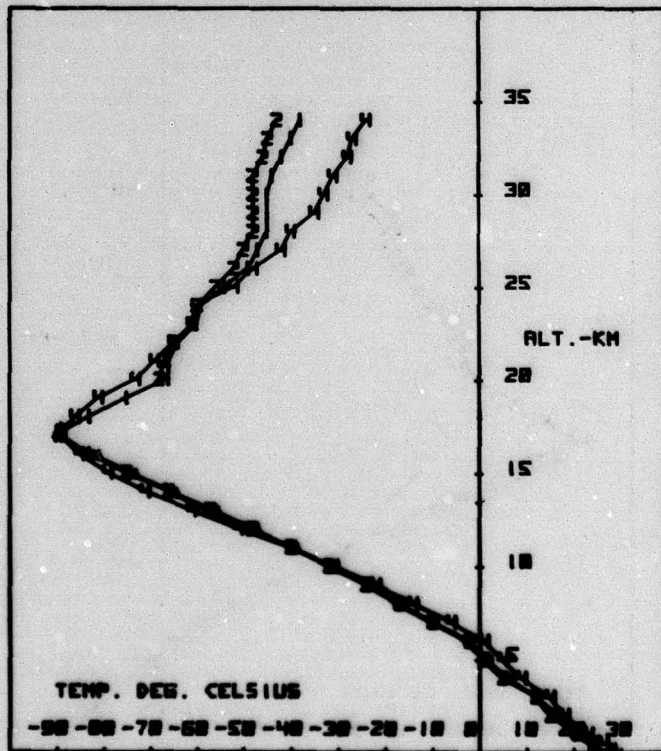


Figure 14. Flight 10; 1-loop mount; 2-TSI thermistor on boom; 4-hygristor thermistor; 6-SWS ramsonde.

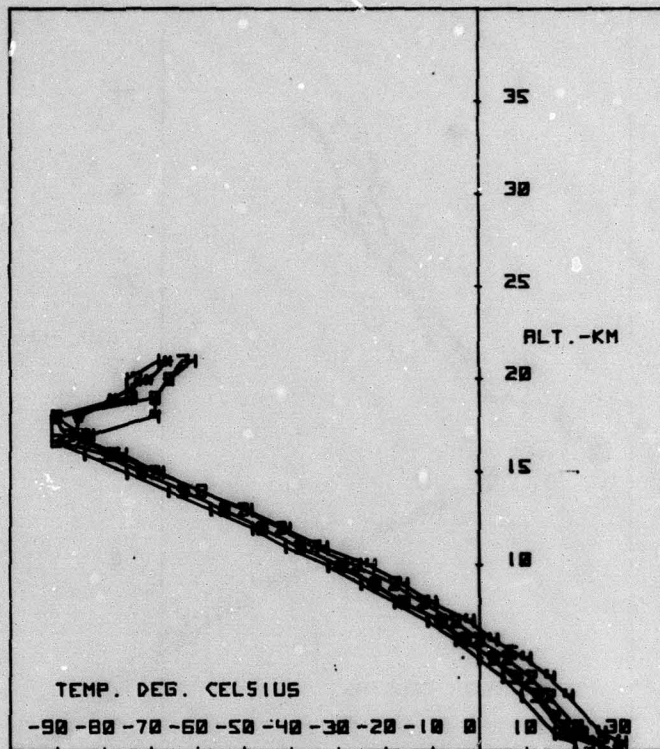


Figure 15. Flight 12; 1-loop mount; 2-post mount on boom; 4-hygristor thermistor; 4-WHS rawinsonde.

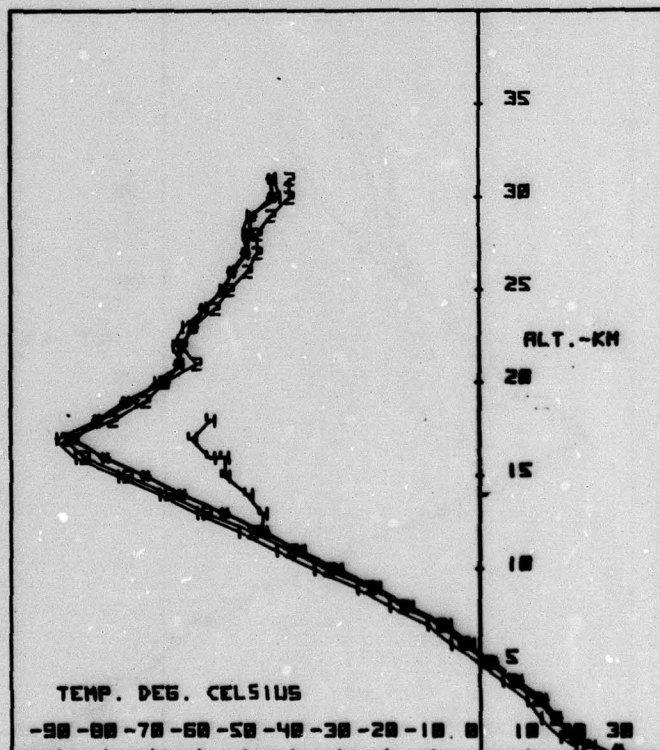


Figure 16. Flight 13; 1-loop mount; 2-Sensi-chip on boom; 3-unfer thermistor on boom; 4-Western thermistor on boom; 4-WHS rawinsonde.

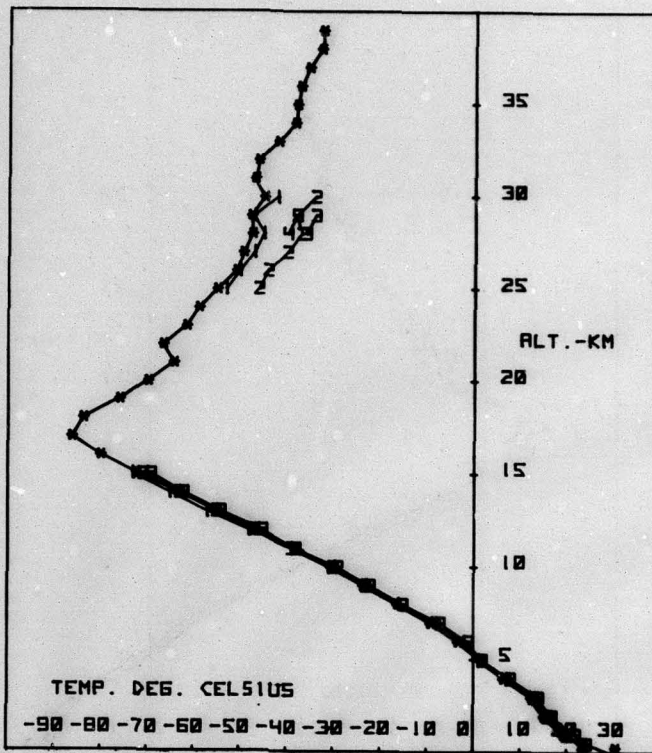


Figure 17. Flight 14; 1-loop mount; 2-standard duct air temperature; 3-standoff standard duct air temperature; 4-standoff C3 duct air temperature; 5-MRS rawinsonde.

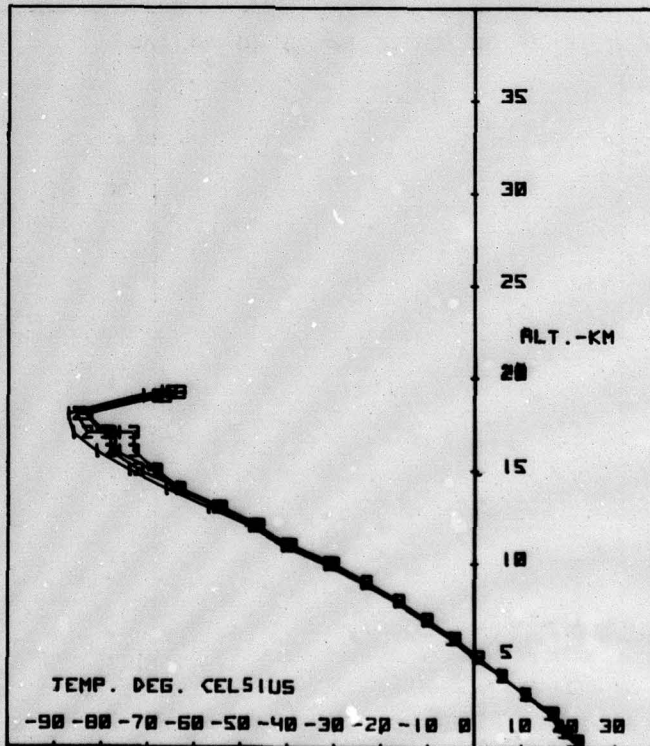


Figure 18. Flight 17; 1-loop mount; 2-standoff duct air temperature; 3-standoff duct inlet temperature; rod thermometer.

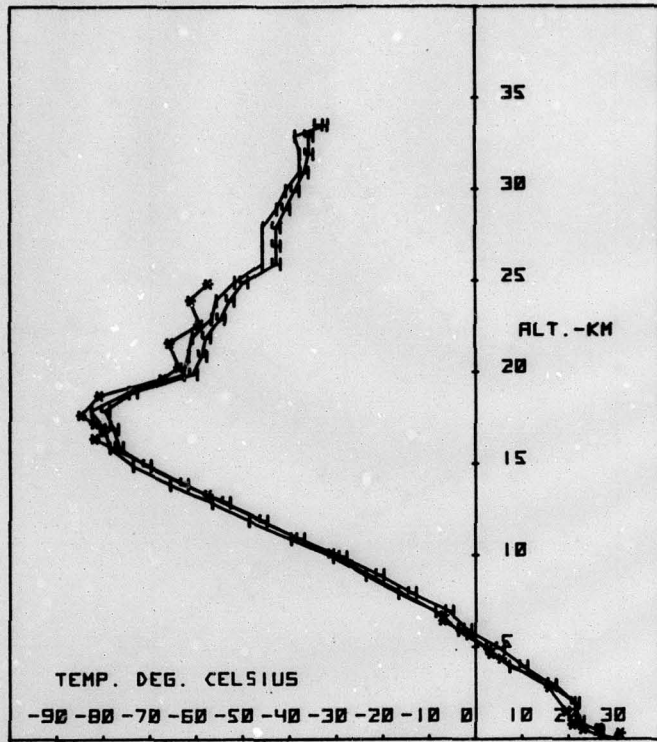


Figure 19. Flight 19; 1-loop mount; 4-rod thermistor; 4-WMS rawinsonde.

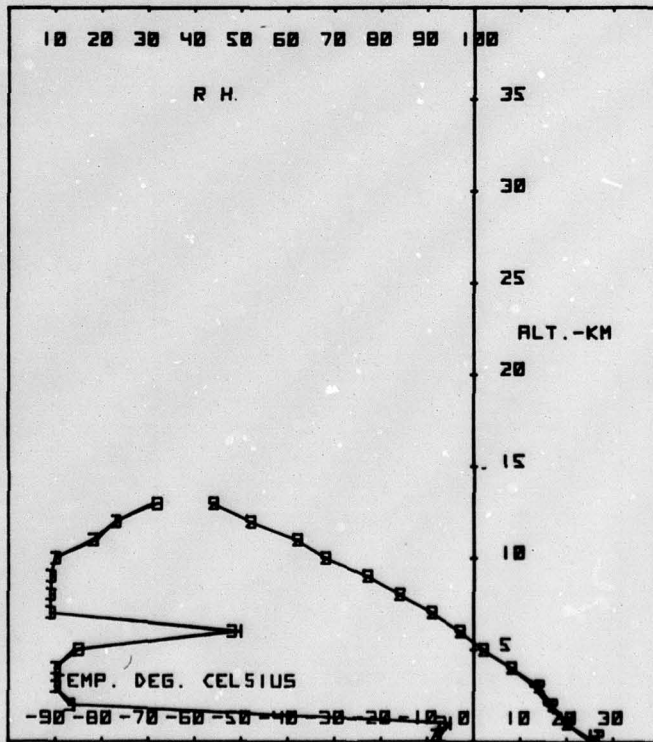


Figure 20. Flight 21; 1-hygriator in standoff duct; 2-hygriator thermistor in standoff duct; 3-hygriator in J005 duct; 4-hygriator thermistor in J005 duct.

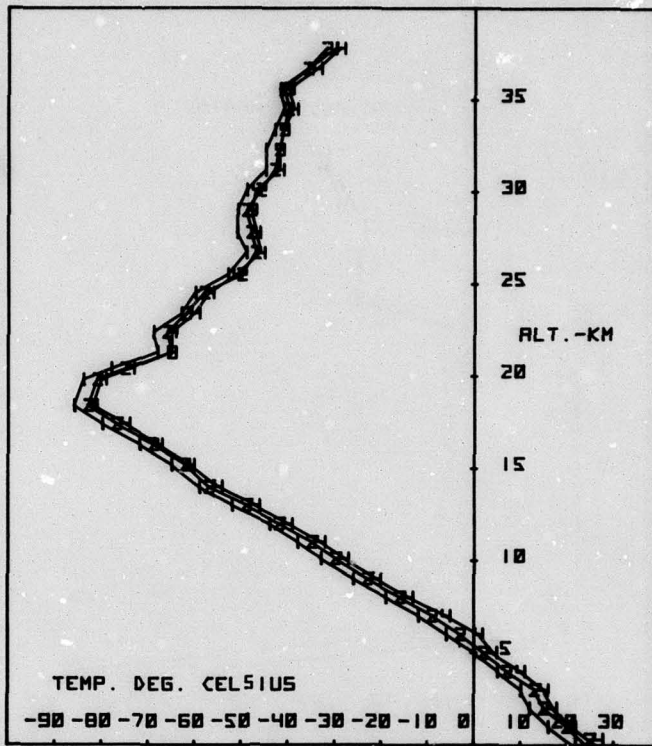


Figure 21. Flight 22; 1-loop mount; 2-post mount thermistor; 4-WSS rod thermistor.

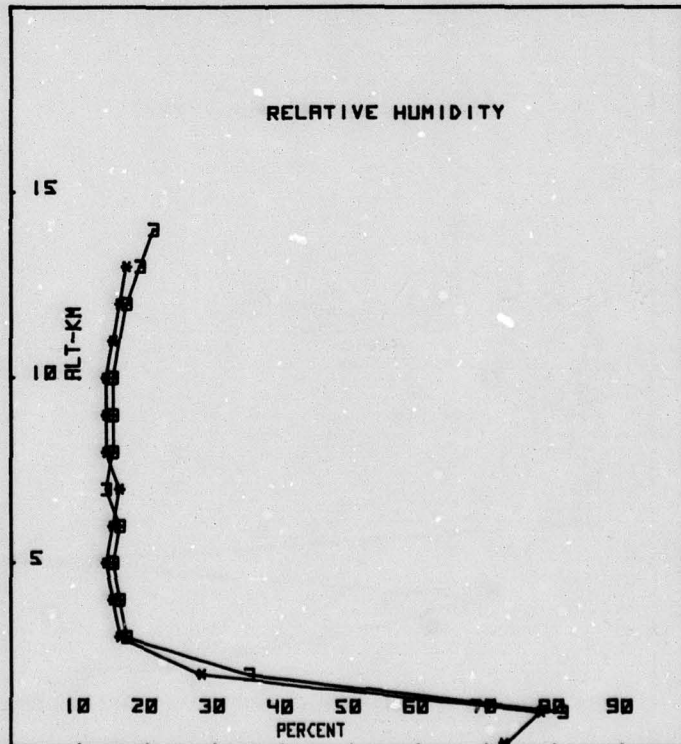


Figure 22. Flight 1; 1-WSS rawinsonde; 3-WSS sonde standard duct.

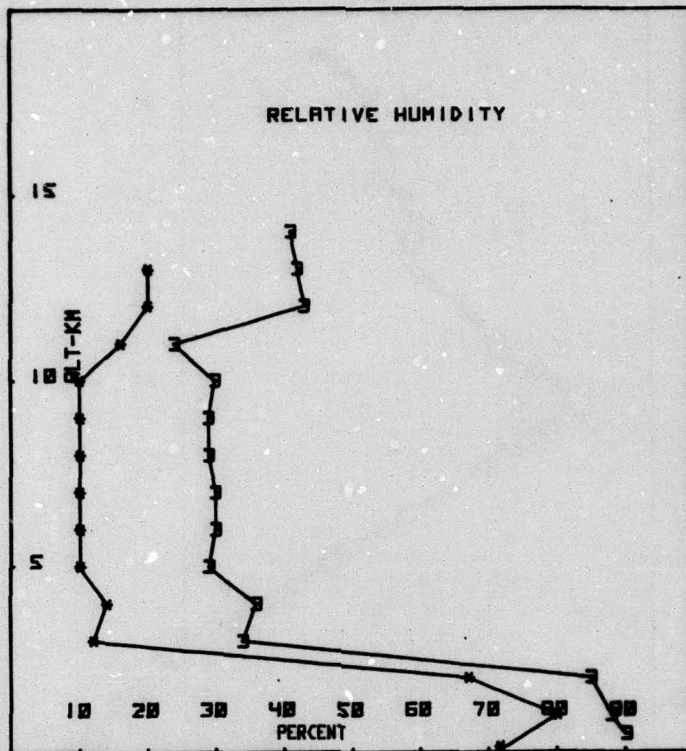


Figure 23. Flight 4; 4-WHS rawinsonde; 3-WHS sonic standard duct at -35 deg angle of attack.

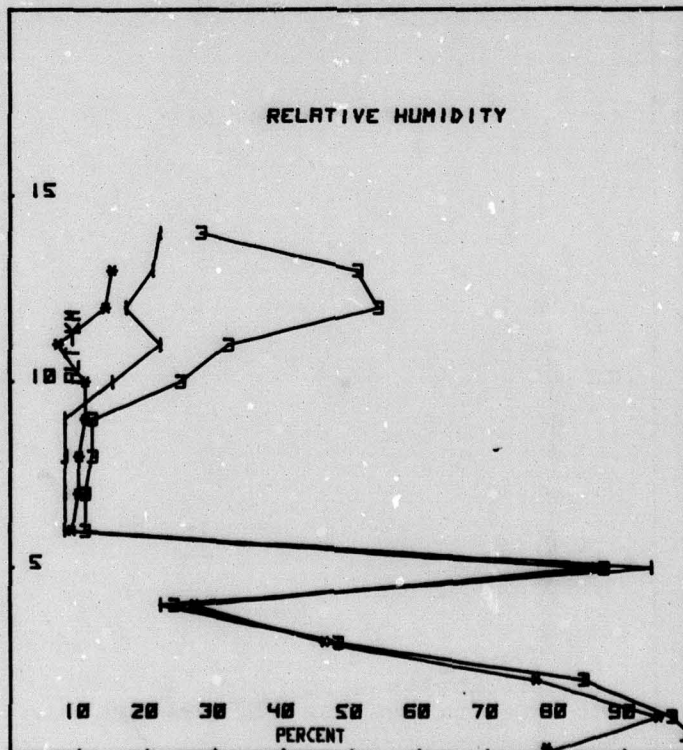


Figure 24. Flight 7; 4-WHS rawinsonde; 1-WHS standard duct with cork and cardboard; 3-O-3 duct tilted at -45 deg.

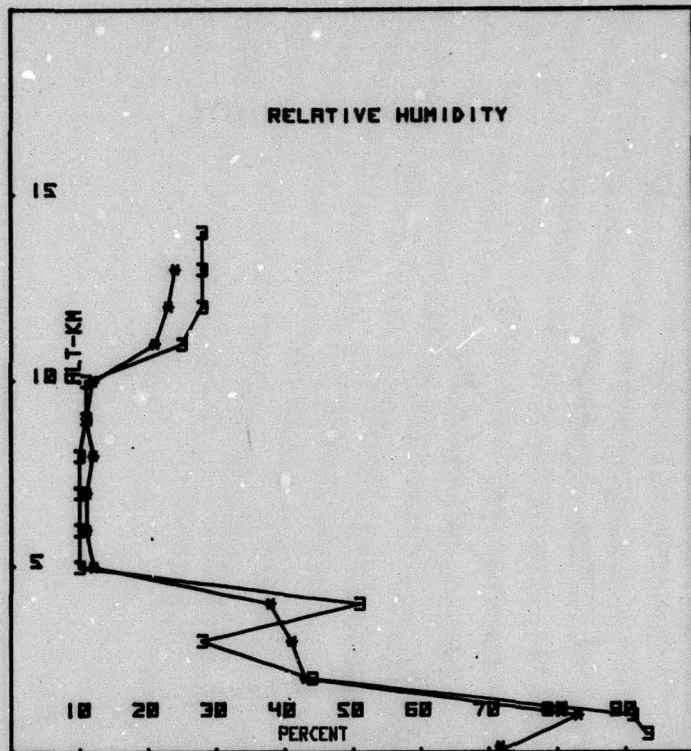


Figure 25. Flight 9; 2-WSS raw/insulated; 3-WSS standard duct with cork and cardboard.

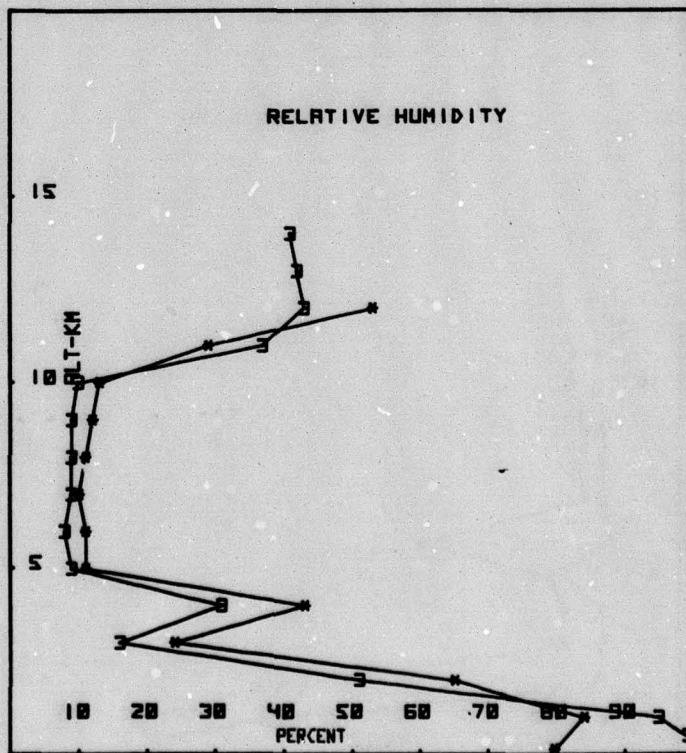


Figure 26. Flight 10; 2-WSS raw/insulated; 3-WSS standard duct without cork and cardboard, night flight.

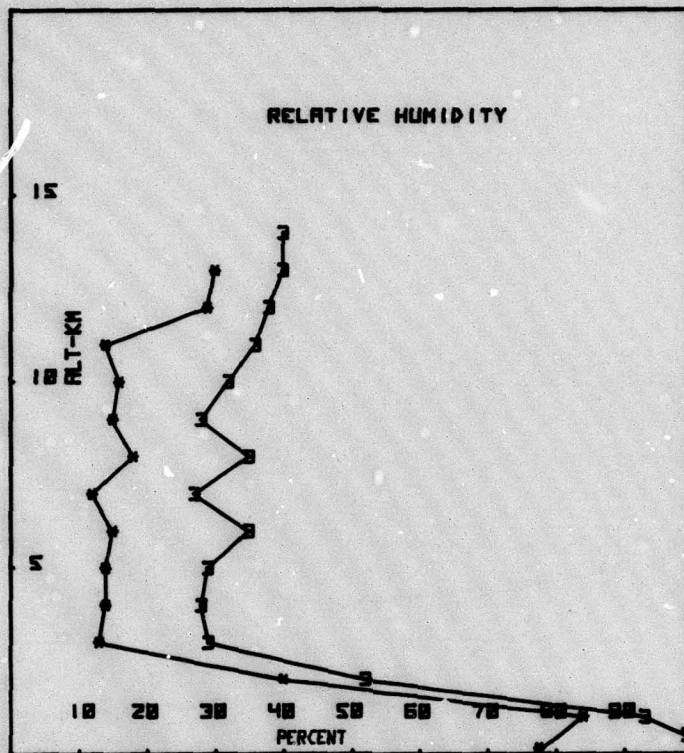


Figure 27. Flight 12; 4-MMS raincoats; 3-MMS standard duct, without cork or shielding.

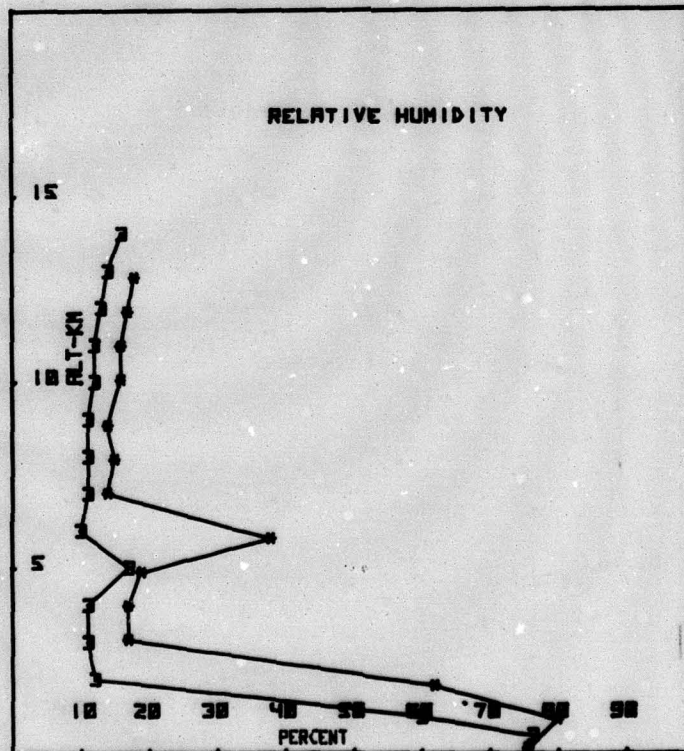


Figure 28. Flight 19; 4-MMS raincoats; 3-standard duct without cork or insulation.

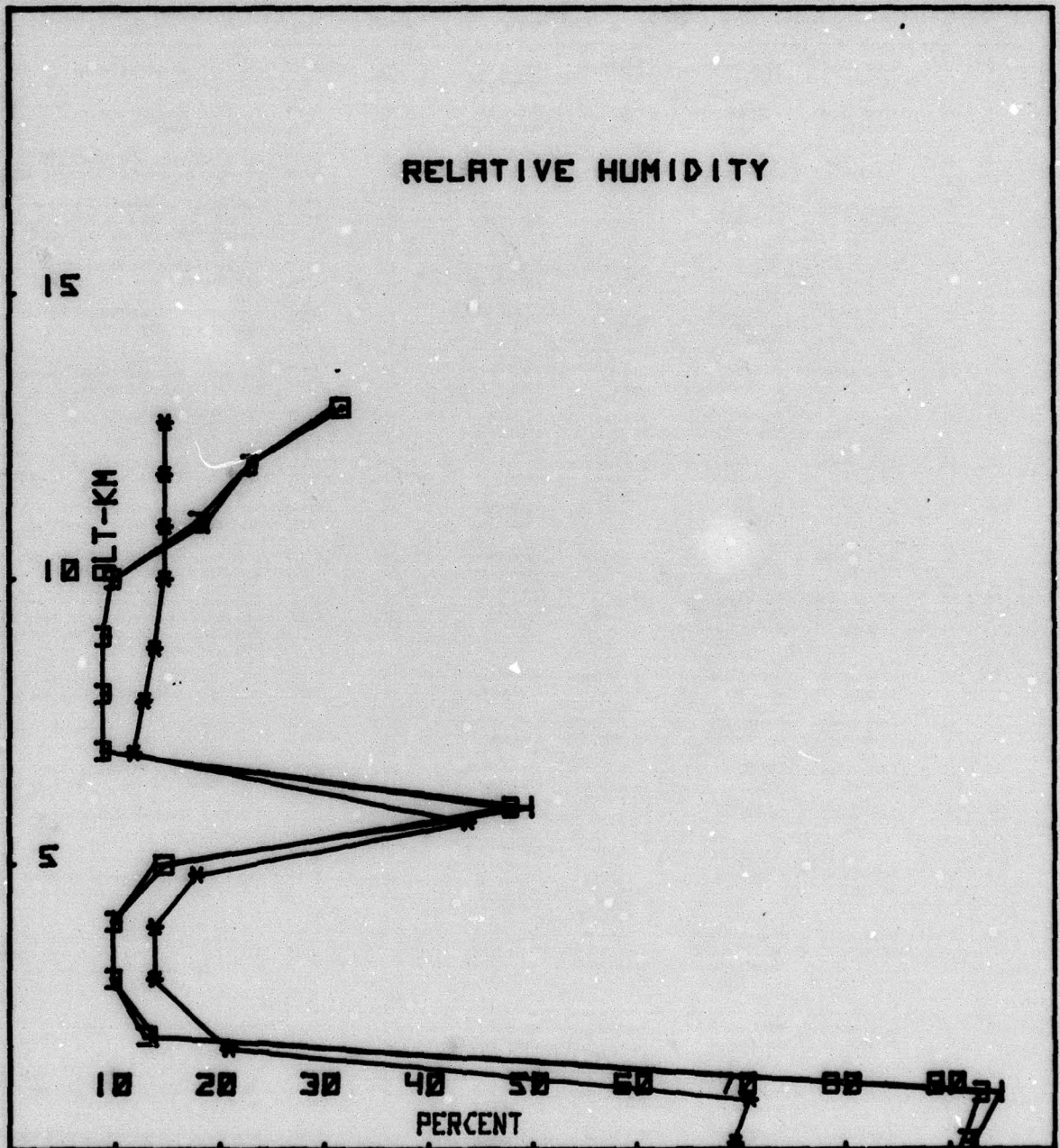


Figure 29. Flight 21; *-NWS rawinsonde; 1-RMS standard duct on standoff, with shielding; 3-NWS duct mounted on side of RMS case.

TABLE 1. RMSS RADIOSONDE FLIGHT TESTS

Flight No.	SN	Channel				Date (1978) Jan	Time	Remarks
		1	2	3	4			
0	1	Loop mount on boom	100K Resistor	Hygristor	Hygristor thermistor	18 18	2220Z 1020L	Std configuration with no modifications.
1	72	Loop mount on boom	100K Resistor	Hygristor	Hygristor thermistor	20 19	0130Z 1330L	Std configuration with no modifications.
2	10	Loop mount on boom	Std duct wall temp	Std duct temp	Add-on std duct temp	20 20	2020Z 0820L	Std sonde with additional std. Std duct adjacent to existing duct.
3	33	Loop mount on boom	Std duct wall temp	Std duct temp	Add-on std duct temp	21 20	0134Z 1334L	Configuration identical to previous flight, but with 6 mm cork between battery and adjacent duct wall.
4	62	Loop mount on boom	100K Resistor	Hygristor	Hygristor thermistor	21 21	2315Z 1115L	Std configuration flown at -35° angle.
5	48	Loop mount on boom	Thermistor at std duct entrance	Std duct temp	Add-on std duct temp	22 21	0332Z 1532L	Std sonde with additional std duct, both at -35° angle.
6	82	Loop mount on boom	C3 inlet thermistor	Std duct temp	C3 duct temp	22 22	2359Z 1159L	Std sonde with additional Krumins both flown at -45° angle.
7	36	Hygristor in std duct	Hygristor thermistor	Hygristor in C3 duct	Hygristor thermistor	23 22	0413Z 1617L	Std sonde at 0° angle plus C3 duct at -45° angle.
8	56	Loop mount on boom	C3 inlet thermistor	Std duct temp	C3 duct temp	23 23	2123Z 0923L	Std sonde plus add-on std duct at -35° plus C3 duct at -45°.
9	45	Loop mount on boom	YSI 44006 on boom	Hygristor	Hygristor thermistor	24 23	0105Z 1305L	Std sonde plus 2nd boom for evaluating YSI 44006 thermistor.
10	50	Loop mount on boom	YSI 44006 on boom	Hygristor	Hygristor thermistor	24 23	0730Z 1930L	Identical to previous flight but launched after dark.
11	52	YSI thermistor on Ch 1/2 IC commutator	YSI thermistor on Ch 3/4 IC commutator	Fixed resistor	Fixed resistor	24 24	1053Z 0653L	Diagnostic flight with YSI thermistors on two IC commutators plus two fixed resistors. Trying to find source of channel loss.
12	58	Loop mount on boom	Post mount on boom	Hygristor	Hygristor thermistor	24 24	2205Z 1005L	Std sonde plus 10-mil bead on post mount adjacent to loop mount.
13	42	Loop mount on boom 1	Sensi chip on boom 1	Wafer therm on boom 2	Western therm on boom 2	25 24	0203Z 1403L	Std sonde with two booms for four thermistors.
14	71	Loop mount on boom	Std duct temp	Standoff std duct temp	Standoff C3 duct temp	25 24	0515Z 1715L	Std sonde with additional std duct and C3 duct on 2-inch standoffs.
15	8	Loop mount on boom	Hygristor	Paralleled with Channel 2	Paralleled with Channel 1	25 24	0823Z 2023L	Std sonde with no modifications.
16	15	Loop mount on boom	Hygristor	Paralleled with Channel 2	Paralleled with Channel 1	26 26	2300Z 1100L	Std sonde with no modifications.
17	67	Loop mount on boom	Standoff duct w/post mount thermistor	Standoff duct inlet thermistor	Rod thermistor	27 26	0152Z 1352L	Std duct mounted on 2-in standoffs. Rod thermistor mounted on VIZ frame work. Balloon burst at 19.2 km.
							<u>Apr</u>	
19	7	Loop mount on boom	Post mount on boom	Hygristor in std duct	NMS rod thermistor	6 6	2230Z 1030L	Channel 2 data not usable.
20	68	Loop mount on boom	Standoff duct hygristor	Std duct hygristor	Standoff duct hygristor thermistor	7 6	0208Z 1408L	Bad ranging; interference between J005 and RMSS; both payloads on same balloon train.
21	57	Hygristor standoff duct	Hygristor thermistor in standoff duct	Hygristor in J005 duct	Hygristor thermistor in J005 duct	7 6	0411Z 1611	J005 duct mounted beside RMSS sonde. Cardboard solar shielding in standoff duct.
22		Loop mount on boom	Post mount on boom	Hygristor in std duct	NMS rod thermistor	7	0857	Nighttime release.

Note: Flight 18 was a standard sonde configuration released for ground equipment test.

TABLE 2. THERMISTORS

Mfg	Type	Size (mm)	Remarks
VEECO	Bead 35A5/7	0.25 (10 mil)	Aluminized; used on loop mount and post mount
VEECO	Wafer 35SC1A604	1.8 x 1.8 x 1.3	Sensi chip, time constant 4 sec
YSI	Bead 44006	1.4 (55 mil)	
YSI	Wafer	2.9 x 1.3 x 0.8	Gold leads 0.05 x 2.9 mm. Same calibration as YSI 44006
Western	Bead PN1M5111-D	1.4 (55 mil)	
VIZ	Bead		Mounted on hygistor

APPENDIX
TABULATED DATA
KWAJALEIN MISSILE RANGE

RMSS RADIOSONDE TEST FLIGHT #1				CONJUNCTIVE RAWINSONDE FOR RMSS FLIGHT #1			
ALT-KM	CH#1	CH#3	CH#4	ALT-KM	TEMP, C	PRESS, MB	RH
1.0	19	81	20	0	29.6	1008.000	72
2.0	16	35	18	1	20.1	900.000	78
3.0	13	17	15	2	16.6	801.000	28
4.0	6	16	7	3	10.6	711.000	16
5.0	0	15	1	4	3.9	630.000	15
6.0	-5	16	-3	5	-1.3	557.000	14
7.0	-11	14	-9	6	-8.2	491.000	15
8.0	-19	15	-17	7	-13.1	431.000	16
9.0	-26	15	-24	8	-19.7	378.000	14
10.0	-33	15	-31	9	-26.7	330.000	14
12.0	-51	17	-47	10	-33.6	287.000	14
13.0	-59	19	-55	11	-41.7	248.000	15
14.0	-69	21	-65	12	-50.2	214.000	16
15.0	999	999	999	13	-58.5	183.000	17
16.0	999	999	999	14	-66.5	156.000	999
17.0	999	999	999	15	-74.7	132.000	999
18.0	999	999	999	16	-79.4	111.000	999
19.0	999	999	999	17	-83.6	92.800	999
20.0	-59	19	-54	18	-84.7	77.600	999
21.0	-55	18	-49	19	-80.4	64.800	999
22.0	-58	17	-45	20	-65.0	54.700	999
23.0	-57	17	-43	21	-60.2	46.600	999
24.0	-55	17	-41	22	-58.0	39.800	999
25.0	-49	16	-36	23	-58.3	34.000	999
26.0	-47	15	-32	24	-56.8	29.100	999
27.0	-47	16	-29	25	-53.6	24.900	999
28.0	-48	15	-26	26	-49.1	21.400	999
29.0	-49	15	-24	27	-48.1	18.400	999
30.0	-46	15	-22	28	-49.3	15.800	999
31.0	-47	17	-19	29	-50.1	13.600	999
32.0	-39	17	-14	30	-47.2	11.700	999
33.0	-36	16	-12	31	-43.3	10.100	999
34.0	-36	17	-10	32	-38.7	8.730	999
35.0	-36	18	-8				

999 DENOTES MISSING DATA

999 DENOTES MISSING DATA

RMSS RADIOSONDE TEST FLIGHT #2					CONJUNCTIVE RAWINSONDE FOR RMSS FLIGHT #2			
ALT-KM	CH#1	CH#2	CH#3	CH#4	ALT-KM	TEMP, C	PRESS, MB	RH
0.5	24	29	36	25	0	28.0	1009.000	78
1.0	20	26	31	22	1	21.0	902.000	79
2.0	16	23	28	18	2	16.6	803.000	28
3.0	13	21	24	15	3	14.1	714.000	14
4.0	6	15	16	7	4	7.5	633.000	13
5.0	-1	11	8	0	5	0.5	560.000	14
6.0	-5	8	5	-3	6	-3.0	494.000	13
7.0	-9	7	0	-7	7	-7.2	435.000	12
8.0	-19	2	-10	-16	8	-15.8	382.000	13
9.0	-26	-2	-17	-24	9	-23.9	334.000	13
10.0	-34	-8	-26	-32	10	-31.1	291.000	14
11.0	-41	-18	-33	-39	11	-39.6	252.000	15
12.0	-50	-24	-42	-47	12	-46.8	218.000	15
13.0	-57	-28	-50	-54	13	-54.6	187.000	14
14.0	-65	-33	-58	-62	14	-62.7	160.000	999
15.0	-73	-37	-67	-71	15	-70.9	135.500	999
16.0	-79	-40	-73	-76	16	-78.6	114.000	999
17.0	-82	-42	-75	-79	17	-81.9	95.800	999
18.0	-84	-42	-77	-81	18	-84.3	80.200	999
18.7	-87	-43	-81	-85	19	-79.7	67.000	999
19.0	-82	-42	-76	-80	20	-63.8	56.600	999
20.0	-65	-31	-58	-61	21	-60.6	48.300	999
21.0	-63	-26	-55	-60	22	-58.8	41.200	999
22.0	-60	-22	-51	-57	23	-57.0	35.200	999
23.0	-59	-19	-47	-53	24	-55.9	30.100	999
24.0	-50	-13	-40	-47	25	-50.8	25.800	999
25.0	-49	-10	-34	-43	26	-49.3	22.200	999
26.0	-47	-8	-32	-42	27	-48.5	19.100	999

999 DENOTES MISSING DATA

RNSS RADIOSONDE TEST FLIGHT #3

ALT-KM	CH#1	CH#2	CH#3	CH#4
0.5	22	27	25	24
1.0	20	24	22	22
2.0	16	20	18	18
3.0	12	17	14	15
4.0	5	10	7	6
5.0	-2	4	0	0
6.0	-7	0	-4	-4
7.0	-12	-4	-10	-10
8.0	-19	-10	-16	-16
9.0	-27	-17	-24	-24
10.0	-34	-22	-30	-30
11.0	-42	-24	-39	-38
12.0	-52	-36	-48	-48
13.0	-57	-41	-53	-54
14.0	-66	-47	-62	-62
15.0	-73	-52	-69	-69
16.0	-81	-57	-74	-75
17.0	-85	-60	-80	-81
18.0	-89	-62	-83	-84
18.4	-90	-62	-85	-85
19.0	-84	-58	-83	-84
20.0	-65	-41	-60	-59
21.0	-63	-39	-58	-56
22.0	-61	-34	-51	-54
23.0	-57	-29	-46	-50
24.0	-54	-24	-42	-46
25.0	-52	-22	-39	-44
26.0	-52	-20	-40	-41
27.0	-53	-16	-39	-43

999 DENOTES MISSING DATA

CONJUNCTIVE RAWINSONDE FOR RNSS FLIGHT #3

ALT-KM	TEMP, C	PRESS, MB	RH
0	30.0	1009.000	69
1	20.6	901.000	61
2	16.5	802.000	41
3	14.1	713.000	17
4	7.5	633.000	18
5	-0.1	560.000	19
6	-4.1	494.000	18
7	-8.5	435.000	18
8	-16.8	382.000	18
9	-24.3	334.000	18
10	-31.3	291.000	19
11	-39.0	252.000	22
12	-47.2	217.000	24
13	-54.8	187.000	24
14	-63.2	159.000	999
15	-71.4	135.000	999
16	-79.3	114.000	999
17	-84.0	95.400	999
18	-86.5	79.700	999
19	-79.4	66.600	999
20	-64.2	56.400	999
21	-61.8	48.000	999
22	-58.0	40.900	999
23	-58.5	35.000	999
24	-53.7	29.900	999
25	-51.6	25.700	999
26	-50.2	22.100	999
27	-50.3	19.000	999
28	-51.6	16.300	999

999 DENOTES MISSING DATA

RNSS RADIOSONDE TEST FLIGHT #4

ALT-KM	CH#1	CH#3	CH#4
0.5	23	90	26
1.0	17	88	21
2.0	12	85	16
3.0	10	34	13
4.0	6	36	9
5.0	-1	29	2
6.0	-6	30	-2
7.0	-11	30	-7
8.0	-19	29	-14
9.0	-26	29	-21
10.0	-32	30	-26
11.0	-37	24	-32
12.0	-48	43	-42
13.0	-58	42	-51
14.0	-69	41	-62
15.0	-79	41	-69
16.0	-86	41	-69
16.7	-90	40	-69
17.0	-88	40	-69
18.0	-80	40	-69
19.0	-71	40	-68
20.0	-70	40	-57
21.0	-59	38	-46
22.0	-58	35	-43
23.0	-59	34	-41
24.0	-57	34	-39
25.0	-55	34	-34

CONJUNCTIVE RAWINSONDE FOR RNSS FLIGHT #4

ALT-KM	TEMP, C	PRESS, MB	RH
0	29.6	1010.000	71
1	20.1	903.000	80
2	15.6	804.000	67
3	12.9	714.000	12
4	7.3	633.000	14
5	1.0	560.000	10
6	-3.2	494.000	10
7	-9.5	435.000	10
8	-15.9	382.000	10
9	-22.9	334.000	10
10	-29.4	291.000	10
11	-38.4	253.000	16
12	-46.3	218.000	20
13	-54.7	187.000	20
14	-63.0	160.000	999
15	-71.4	136.000	999
16	-80.4	114.000	999
17	-87.7	95.500	999
18	-82.8	79.700	999
19	-79.1	67.000	999
20	-68.3	56.600	999
21	-60.3	48.100	999
22	-57.1	41.100	999
23	-56.6	35.200	999
24	-56.2	30.100	999
25	-54.3	25.700	999

999 DENOTES MISSING DATA

RMSS RADIOSONDE TEST FLIGHT #5

ALT-KM	CH#1	CH#2	CH#3	CH#4
0.5	21	19	25	19
1.0	19	17	21	16
2.0	15	13	17	11
3.0	11	8	14	5
4.0	7	5	10	2
5.0	0	-2	2	-6
6.0	-3	-6	0	-9
7.0	-9	-11	-6	-15
8.0	-13	-16	-9	-20
9.0	-22	-24	-18	-27
10.0	-32	-34	-30	-36
11.0	-41	-44	-38	-44
12.0	-51	-54	-48	-53
13.0	-60	-63	-59	-59
14.0	-67	-70	-65	-64
15.0	-78	-77	-72	-71
16.0	-86	-81	-81	-75
16.8	-88	-89	-87	-78
17.0	-87	-82	-78	-75
18.0	-80	-76	-75	-72
19.0	-68	-64	-59	-64
20.0	-67	-63	-57	-63
21.0	-60	-53	-45	-56
22.0	-60	-61	-55	-57
23.0	-59	-51	-49	-55
24.0	-56	-55	-41	-54
25.0	-53	-43	-35	-50
26.0	-53	-37	-33	-45
27.0	-50	-41	-29	-47
28.0	-46	-38	-36	-46
29.0	-46	-32	-19	-43
30.0	-42	-35	-30	-42
31.0	-40	-41	-26	-40
32.0	-40	-35	-28	-41
33.0	-37	-39	-25	-40
34.0	-34	-30	-13	-35
35.0	-29	-30	-18	-35

CONJUNCTIVE RAWINSONDE FOR RMSS FLIGHT #5

ALT-KM	TEMP, C	PRESS, MB	RH
0	28.8	1007.000	72
1	19.7	900.000	89
2	16.8	801.000	54
3	12.0	712.000	71
4	8.0	632.000	18
5	1.3	559.000	12
6	-3.1	493.000	11
7	-9.0	434.000	11
8	-15.7	381.000	11
9	-22.3	334.000	12
10	-30.3	291.000	13
11	-37.4	252.000	15
12	-45.6	218.000	21
13	-53.4	187.000	23
14	-61.6	160.000	999
15	-70.6	136.000	999
16	-78.3	115.000	999
17	-86.5	95.900	999
18	-87.5	79.900	999
19	-78.2	67.000	999
20	-68.1	56.500	999
21	-63.8	48.000	999
22	-60.1	40.900	999
23	-59.6	34.900	999
24	-57.1	29.800	999
25	-52.7	25.500	999
26	-53.8	21.900	999
27	-52.2	18.800	999
28	-49.5	16.100	999
29	-46.8	13.900	999
30	-44.4	12.000	999
31	-42.8	10.300	999
32	-42.7	8.920	999

999 DENOTES MISSING DATA

RMSS RADIOSONDE TEST FLIGHT #6

ALT-KM	CH#1	CH#2	CH#3	CH#4
0.5	23	25	28	23
1.0	19	23	24	21
2.0	15	19	20	17
3.0	10	14	16	11
4.0	6	11	11	7
5.0	1	6	5	2
6.0	-2	3	4	0
7.0	-10	-6	-5	-8
8.0	-18	-14	-12	-16
9.0	-25	-21	-17	-22
10.0	-32	-29	-25	-30
11.0	-40	-36	-36	-37
12.0	-47	-43	-38	-42
13.0	-55	-53	-51	-52
14.0	-64	-63	-49	-49
15.0	-70	-67	-55	-52
16.0	-87	-87	999	-35
17.0	-88	-82	999	999
18.0	-81	-77	999	999
19.0	-81	-77	999	999
20.0	-69	-63	-55	999
21.0	-63	-61	-50	999
22.0	-59	-54	999	999
23.0	-58	-56	-44	999
24.0	-57	-48	999	999
25.0	-55	-52	999	999
26.0	-52	-50	999	999
27.0	-46	-45	999	999

999 DENOTES MISSING DATA

CONJUNCTIVE RAWINSONDE FOR RMSS FLIGHT #6

ALT-KM	TEMP, C	PRESS, MB	RH
0	31.8	1009.000	74
1	19.8	901.000	99
2	15.9	803.000	97
3	11.8	713.000	63
4	6.6	633.000	79
5	1.6	560.000	75
6	-3.0	494.000	9
7	-10.1	435.000	9
8	-16.7	382.000	10
9	-23.2	334.000	10
10	-31.0	291.000	11
11	-39.4	252.000	12
12	-46.3	218.000	12
13	-54.3	187.000	13
14	-62.9	160.000	999
15	-71.4	135.000	999
16	-78.7	114.000	999
17	-86.8	95.500	999
18	-83.9	79.600	999
19	-80.1	66.800	999
20	-69.6	56.300	999
21	-62.0	47.900	999
22	-59.2	40.800	999
23	-58.0	34.900	999
24	-57.6	29.800	999
25	-56.9	25.500	999
26	-53.3	21.800	999
27	-51.8	18.700	999

999 DENOTES MISSING DATA

RMS RADIOSONDE TEST FLIGHT #7

ALT-KM	CH#1	CH#2	CH#3	CH#4
0.5	100	26	101	26
1.0	97	24	97	24
2.0	84	20	84	20
3.0	48	16	48	16
4.0	22	10	24	10
5.0	94	3	87	3
6.0	8	1	11	0
7.0	8	-5	11	-6
8.0	8	-12	12	-13
9.0	8	-20	12	-21
10.0	15	-29	25	-29
11.0	22	-38	32	-38
12.0	17	-47	54	-48
13.0	21	-60	51	-60
14.0	22	-72	28	-15
15.0	23	-79	29	-16
16.0	23	-85	30	-57
17.0	24	-87	31	-84
18.0	23	-84	30	-81
19.0	23	-78	30	-77
20.0	20	-67	29	-67
21.0	18	-60	27	-62
22.0	16	-59	26	-61
23.0	15	-55	25	-56
24.0	13	-50	23	-51
25.0	12	-46	18	-47
26.0	11	-42	16	-45
27.0	17	-37	15	-42
28.0	9	-32	14	-38
29.0	9	-29	14	-34
30.0	8	-27	14	-33
31.0	8	-25	13	-29
32.0	8	-21	13	-25
33.0	8	-18	12	-23
34.0	8	-17	12	-22
35.0	8	-15	13	-21
36.0	8	-13	12	-20
37.0	8	-13	12	-19

CONJUNCTIVE RAWINSONDE FOR RMS FLIGHT #7

ALT-KM	TEMP, C	PRESS, MB	RH
0	27.5	1006.000	78
1	19.3	898.000	95
2	16.0	800.000	77
3	11.8	711.000	46
4	5.3	630.000	27
5	-1.4	557.000	85
6	-3.7	492.000	9
7	-11.3	433.000	10
8	-17.7	379.000	10
9	-24.1	332.000	11
10	-31.8	289.000	11
11	-39.8	250.000	7
12	-47.2	216.000	14
13	-54.7	185.000	15
14	-63.3	158.000	999
15	-71.4	134.000	999
16	-79.2	113.000	999
17	-87.8	94.600	999
18	-84.0	78.800	999
19	-80.9	66.000	999
20	-72.4	55.600	999
21	-64.6	47.200	999
22	-61.7	40.200	999
23	-61.3	34.200	999
24	-58.6	29.200	999
25	-56.1	24.990	999
26	-53.4	21.400	999
27	-51.5	18.400	999
28	-49.5	15.800	999
29	-47.7	13.600	999
30	-46.4	11.700	999
31	-45.0	10.100	999
32	-44.2	8.700	999
33	-39.6	7.520	999
34	-39.3	6.510	999
35	-39.3	5.640	999
36	-39.5	4.880	999
37	-38.7	4.230	999

999 DENOTES MISSING DATA

RMS RADIOSONDE TEST FLIGHT #8

ALT-KM	CH#1	CH#3	CH#4
1.0	17	21	21
2.0	14	17	17
3.0	10	13	13
4.0	4	8	6
5.0	0	3	2
6.0	-6	-3	-3
7.0	-12	-9	-9
8.0	-18	-15	-16
9.0	-24	-20	-21
10.0	-34	-30	-30
11.0	-42	-39	-39
12.0	-51	-46	-48
13.0	-60	-57	-57
14.0	-69	-63	-64
15.0	-76	-71	-71
16.0	-84	-78	-79
16.8	-91	-87	-85
17.0	-91	-82	-81
18.0	-85	-77	-85
19.0	999	-66	-67
20.0	999	-60	-63
21.0	-65	-53	-49
22.0	-61	-49	-50
23.0	-56	-51	-47
24.0	-58	-46	-44
25.0	-54	-46	-47
26.0	-34	-45	-42
27.0	-32	-48	-40
28.0	-50	-44	-36
29.0	-46	-37	-32
30.0	-44	-34	-31
31.0	-45	-31	-24
32.0	-45	-36	-23
33.0	-42	-30	-25
34.0	-38	-30	-19
35.0	-37	-14	-19
36.0	-31	-15	-15

CONJUNCTIVE RAWINSONDE FOR RMS FLIGHT #8

ALT-KM	TEMP, C	PRESS, MB	RH
0	31.1	1009.000	75
1	21.2	902.000	83
2	17.1	803.000	78
3	12.7	714.000	48
4	6.6	634.000	43
5	2.3	561.000	30
6	-3.0	495.000	10
7	-8.4	436.000	9
8	-15.2	383.000	10
9	-21.0	335.000	10
10	-29.1	292.000	11
11	-37.2	254.000	48
12	-45.6	219.000	50
13	-54.4	188.000	51
14	-63.1	161.000	999
15	-71.3	136.000	999
16	-78.5	115.000	999
17	-87.5	96.200	999
18	-82.4	80.200	999
19	-77.3	67.200	999
20	-67.2	56.800	999
21	-64.6	48.300	999
22	-61.7	41.100	999
23	-58.8	35.100	999
24	-56.2	30.000	999
25	-55.6	25.700	999
26	-52.7	22.000	999
27	-51.4	18.900	999
28	-49.1	16.200	999
29	-45.6	14.000	999
30	-43.7	12.100	999
31	-42.9	10.400	999
32	-41.7	8.990	999
33	-41.9	7.770	999
34	-39.9	6.720	999
35	-37.4	5.820	999
36	-34.0	5.050	999

999 DENOTES MISSING DATA

RMSS RADIOSONDE TEST FLIGHT #9

ALT-KM	CH#1	CH#2	CH#3	CH#4
0.5	23	25	93	27
1.0	18	21	91	23
2.0	15	18	44	21
3.0	10	13	28	16
4.0	4	7	51	10
5.0	0	3	10	6
6.0	-6	-4	10	0
7.0	-12	-10	10	-6
8.0	-19	-17	10	-13
9.0	-25	-23	11	-20
10.0	-34	-32	11	-30
11.0	-42	-39	25	-39
12.0	-50	-48	28	-49
13.0	-59	-57	28	-59
14.0	-68	-66	28	-69
15.0	-75	-73	29	-74
16.0	-83	-78	30	-76
16.5	-86	999	28	999
17.0	-89	999	999	999
18.4	-85	-77	999	999
19.0	-70	-68	999	999
20.0	-67	-62	999	999
21.0	-66	-61	999	999
22.0	-63	-57	999	999
23.0	-59	-55	999	999
24.0	-59	-54	999	999
25.0	-57	-52	999	999
26.0	-54	-48	999	999
27.0	-51	-44	999	999
28.0	-47	-41	999	999
29.0	-46	-39	999	999
30.0	-44	-37	999	999
31.0	-45	-37	999	999
32.0	-44	-35	999	999
33.0	-43	-34	999	999
34.0	-38	-30	999	999

999 DENOTES MISSING DATA

CONJUNCTIVE RAWINSONDE FOR RMSS FLIGHT #9

ALT-KM	TEMP, C	PRESS, MB	RH
0	29.4	1008.000	71
1	19.8	900.000	83
2	16.4	801.000	43
3	11.9	712.000	41
4	6.3	631.000	38
5	1.7	559.000	12
6	-4.0	493.000	11
7	-9.9	434.000	11
8	-16.6	381.000	12
9	-23.1	333.000	11
10	-30.4	290.000	12
11	-38.5	252.000	21
12	-46.2	217.000	23
13	-55.0	187.000	24
14	-63.3	159.000	999
15	-70.6	135.000	999
16	-78.7	114.000	999
17	-86.5	95.300	999
18	-84.7	79.500	999
19	-74.3	66.700	999
20	-69.0	56.500	999
21	-64.5	47.900	999
22	-61.6	40.800	999
23	-60.2	34.800	999
24	-58.1	29.700	999
25	-55.2	25.400	999
26	-54.1	21.800	999
27	-50.9	18.700	999
28	-46.1	16.100	999
29	-42.3	13.900	999
30	-43.2	12.000	999
30	-44.6	10.300	999
32	-44.8	8.920	999
33	-40.8	7.700	999
34	-37.7	6.670	999

999 DENOTES MISSING DATA

RMSS RADIOSONDE TEST FLIGHT #10

ALT-KM	CH#1	CH#2	CH#3	CH#4
0.5	23	24	99	26
1.0	20	21	95	23
2.0	17	15	51	18
3.0	12	12	16	15
4.0	5	5	31	9
5.0	1	1	9	5
6.0	-3	-2	8	1
7.0	-10	-10	9	-6
8.0	-17	-17	9	-14
9.0	-24	-24	9	-22
10.0	-32	-32	10	-31
11.0	-40	-40	37	-40
12.0	-49	-48	43	-51
13.0	-58	-57	42	-61
14.0	-66	-66	41	-71
15.0	-75	-75	41	-79
16.0	-83	999	40	-85
17.0	-89	999	40	-89
17.2	-89	999	40	-89
18.0	-83	999	40	-86
19.0	-75	999	40	-81
20.0	-66	-68	38	-73
21.0	-66	-67	34	-69
22.0	-64	-65	33	-65
23.0	-60	-61	29	-61
24.0	-59	-60	29	-60
25.0	-54	-56	22	-52
26.0	-49	-52	16	-48
27.0	-47	-50	13	-42
28.0	-45	-48	12	-40
29.0	-45	-48	12	-35
30.0	-45	-48	12	-33
31.0	-44	-48	13	-31
32.0	-42	-46	13	-28
33.0	-40	-45	13	-27
34.0	-38	-43	15	-24

999 DENOTES MISSING DATA

CONJUNCTIVE RAWINSONDE FOR RMSS FLIGHT #10

ALT-KM	TEMP, C	PRESS, MB	RH
0	27.2	1008.000	79
1	20.2	900.000	84
2	16.1	801.000	65
3	12.1	711.000	24
4	6.3	631.000	43
5	1.7	558.000	11
6	-2.4	493.000	11
7	-9.9	434.000	10
8	-17.2	381.000	11
9	-23.7	333.000	12
10	-31.2	290.000	13
11	-39.3	251.000	29
12	-47.6	217.000	53
13	-56.1	186.000	999
14	-65.0	159.000	999
15	-73.7	134.000	999
16	-81.6	113.000	999
17	-89.8	94.300	999

999 DENOTES MISSING DATA

RMSS RADIOSONDE TEST FLIGHT #12

CONJUNCTIVE RAWINSONDE FOR RMSS FLIGHT #12

ALT-KM	CH#1	CH#2	CH#3	CH#4	ALT-KM	TEMP, C	PRESS, MB	RH
0.5	20	22	99	23	0	28.1	1009.000	77
1.0	17	20	93	20	1	19.7	901.000	84
2.0	13	16	52	16	2	16.1	802.000	40
3.0	10	12	29	13	3	13.1	713.000	13
4.0	5	7	28	8	4	8.0	632.000	14
5.0	0	2	29	2	5	2.6	559.000	14
6.0	-6	-3	35	-2	6	-3.6	494.000	15
7.0	-11	-8	27	-7	7	-8.2	435.000	12
8.0	-19	-16	35	-15	8	-15.8	382.000	18
9.0	-26	-23	28	-22	9	-22.4	334.000	15
10.0	-35	-32	32	-30	10	-30.3	291.000	16
11.0	-43	-40	36	-38	11	-38.6	253.000	14
12.0	-51	-48	38	-46	12	-45.9	218.000	29
13.0	-60	-58	40	-46	13	-54.5	187.000	30
14.0	-68	-66	40	-49	14	-63.6	160.000	999
15.0	-77	-75	40	-54	15	-71.5	136.000	999
16.0	-86	-84	40	-54	16	-80.0	114.000	999
16.0	-86	-84	40	-57	17	-86.8	95.400	999
17.0	-90	-88	40	-61	18	-81.6	79.700	999
18.0	-81	-78	40	-57	19	-75.6	66.900	999
19.0	-73	-71	999	999	20	-67.0	56.600	999
20.0	-69	-67	999	999	21	-64.2	48.100	999
21.0	-63	-60	999	999	22	-63.5	40.900	999
22.0	-65	-63	999	999	23	-61.0	34.900	999
23.0	-63	-61	999	999	24	-58.8	29.740	999
24.0	-58	-56	999	999	25	-54.5	25.500	999
25.0	-55	-53	999	999	26	-52.7	21.800	999
26.0	-52	-49	999	999	27	-49.8	18.700	999
27.0	-49	-47	999	999	28	-48.8	16.100	999
28.0	-50	-47	999	999	29	-48.4	13.900	999
29.0	-49	-44	999	999	30	-44.0	12.000	999
30.0	-42	-40	999	999	31	-44.2	10.300	999
31.0	-43	-40	999	999				

999 DENOTES MISSING DATA

999 DENOTES MISSING DATA

RMSS RADIOSONDE TEST FLIGHT #13

CONJUNCTIVE RAWINSONDE FOR RMSS FLIGHT #13

ALT-KM	CH#1	CH#2	CH#3	CH#4	ALT-KM	TEMP, C	PRESS, MB	RH
0.5	23	23	24	23	0	29.5	1007.000	72
1.0	20	20	22	20	1	19.4	899.000	87
2.0	16	16	17	16	2	15.2	800.000	36
3.0	13	13	14	13	3	12.4	711.000	18
4.0	7	8	8	7	4	6.4	630.000	19
5.0	1	2	2	1	5	1.6	558.000	21
6.0	-2	-1	-1	-1	6	-3.3	492.000	21
7.0	-8	-7	-7	-8	7	-9.2	434.000	15
8.0	-16	-15	-15	-15	8	-16.3	380.000	17
9.0	-23	-22	-23	-22	9	-23.6	333.000	16
10.0	-31	-29	-30	-30	10	-30.6	290.000	31
11.0	-39	-38	-39	-38	11	-38.2	251.000	52
12.0	-48	-45	-47	-45	12	-46.7	217.000	58
13.0	-57	-54	-55	-54	13	-55.1	186.000	53
14.0	-65	-62	-63	-62	14	-63.2	159.000	999
15.0	-73	-69	-71	-69	15	-72.2	135.000	999
25.0	-53	-46	999	999	16	-80.0	113.000	999
26.0	-50	-44	999	999	17	-86.3	94.900	999
27.0	-47	-40	99	999	18	-83.8	79.000	999
28.0	-45	-37	-36	-40	19	-76.0	66.500	999
29.0	-47	-38	-34	-38	20	-69.9	56.200	999
30.0	-42	-34	999	999	21	-64.3	47.600	999
					22	-66.6	40.500	999
					23	-61.5	34.400	999
					24	-58.9	29.400	999
					25	-55.0	25.100	999
					26	-50.8	21.600	999
					27	-49.5	18.500	999
					28	-47.6	16.000	999
					29	-47.8	13.700	999
					30	-45.0	11.800	999
					31	-47.0	10.200	999
					32	-46.3	8.790	999
					33	-42.1	7.580	999
					34	-38.5	6.560	999
					35	-38.1	5.690	999
					36	-37.3	4.930	999
					37	-35.5	4.270	999
					38	-32.9	3.710	999
					39	-32.7	3.230	999

999 DENOTES MISSING DATA

999 DENOTES MISSING DATA

RMSS RADIOSONDE TEST FLIGHT #14

ALT-KM	CH#1	CH#2	CH#3	CH#4
0.5	20	26	23	30
1.0	16	22	18	26
3.0	9	15	12	19
4.0	5	11	7	15
5.0	0	6	3	10
6.0	-5	0	-3	3
7.0	-11	-5	-8	-2
8.0	-18	-12	-16	-10
9.0	-25	-18	-22	-16
10.0	-32	-26	-29	-23
11.0	-41	-35	-38	-33
12.0	-48	-42	-46	-41
13.0	-57	-50	-54	-49
14.0	-66	-59	-63	-59
15.0	-75	-69	-72	-68
16.0	-84	-78	-80	-76
16.7	-91	-85	-90	-84
17.0	-91	-84	-88	-83
18.0	-91	-90	-90	-69
19.0	-75	-69	-74	-69
20.0	-75	-66	-73	-66
21.0	-68	-63	-44	-61

CONJUNCTIVE RAWINSONDE FOR RMSS FLIGHT #14

ALT-KM	TEMP, C	PRESS, MB	RH
0	28.5	1006.000	69
1	19.7	898.000	83
2	15.9	799.000	40
3	12.5	710.000	15
4	8.0	630.000	21
5	2.9	558.000	31
6	-3.6	493.000	74
7	-8.5	434.000	15
8	-16.2	381.000	18
9	-22.6	333.000	12
10	-29.8	290.000	20
11	-38.0	252.000	65
12	-46.0	218.000	68
13	-54.3	187.000	52
14	-62.8	160.000	999
15	-72.0	135.000	999
16	-79.0	114.000	999
17	-86.1	95.400	999
18	-85.5	79.600	999
19	-78.3	66.600	999
20	-70.6	56.300	999
21	-66.4	47.600	999

999 DENOTES MISSING DATA

RMSS RADIOSONDE TEST FLIGHT #17

ALT-KM	CH#1	CH#2	CH#3	CH#4
0.5	22	22	21	22
1.0	19	20	19	19
2.0	16	17	16	17
3.0	11	11	11	11
4.0	6	6	6	6
5.0	0	1	1	1
6.0	-5	-4	-5	-4
7.0	-11	-10	-10	-10
8.0	-17	-16	-16	-16
9.0	-24	-23	-23	-23
10.0	-32	-30	-31	-31
11.0	-41	-39	-40	-40
12.0	-48	-47	-46	-48
13.0	-57	-55	-54	-55
14.0	-66	-63	-63	-64
15.0	-74	-72	-68	-69
16.0	-81	-78	-73	-77
17.0	-86	-83	-79	-80
18.0	-87	-85	-83	-83
19.0	-71	-68	-66	-68
19.2	-67	-65	-63	-65

CONJUNCTIVE RAWINSONDE FOR RMSS FLIGHT #17

ALT-KM	TEMP, C	PRESS, MB	RH
0	29.4	1007.000	67
1	19.9	899.000	81
2	17.7	800.000	19
3	12.5	712.000	48
4	6.8	631.000	35
5	1.9	559.000	10
6	-3.5	493.000	9
7	-9.8	434.000	10
8	-15.7	381.000	10
9	-22.4	333.000	14
10	-29.1	291.000	15
11	-38.0	252.000	17
12	-46.1	218.000	19
13	-54.4	187.000	19
14	-62.8	160.000	999
15	-70.7	136.000	999
16	-78.4	114.000	999
17	-83.5	95.700	999
18	-88.4	79.900	999
19	-74.1	66.800	999

999 DENOTES MISSING DATA

RMSS RADIOSONDE TEST FLIGHT #19

ALT-KM	CH#1	CH#3	CH#4
0.5	26	76	26
1.0	22	60	22
2.0	21	12	21
3.0	17	11	16
4.0	7	11	10
5.0	2	17	5
6.0	-4	10	-2
7.0	-9	11	-6
8.0	-17	11	-14
9.0	-24	11	-21
10.0	-31	12	-29
11.0	-40	12	-38
12.0	-49	13	-46
13.0	-57	14	-54
14.0	-66	16	-63
15.0	-74	16	-71
16.0	-79	18	-77
17.0	-80	18	-78
18.0	-83	19	-80
19.0	-75	17	-74
20.0	-63	15	-61
21.0	-62	15	-59
22.0	-61	14	-58
23.0	-57	14	-55
24.0	-56	14	-53
25.0	-52	13	-50
26.0	-46	13	-43
27.0	-46	12	-43
28.0	-46	13	-43
29.0	-43	12	-41
30.0	-41	12	-39
31.0	-38	12	-37
32.0	-38	12	-36
33.0	-39	12	-36
33.6	-32	14	-34

RMSS RADIOSONDE TEST FLIGHT #20

ALT-KM	CH#1	CH#2	CH#3	CH#4
1.2	23	64	67	23
1.3	19	65	68	20
1.6	19	44	47	20
1.8	18	29	31	19
2.1	18	23	26	19
2.9	18	14	18	17
3.1	17	13	16	16
3.3	16	9	11	15
5.7	999	55	999	999
6.2	999	66	58	999
6.4	-2	54	59	-2
6.5	-4	48	56	999
6.8	999	999	999	999
7.8	-14	4	6	-14
8.4	-18	2	5	-18
9.3	-26	7	8	-24
9.5	-28	11	17	-25
9.7	-29	15	22	-26
9.8	-31	15	22	-27
9.9	-32	16	22	-28
10.1	-34	16	23	-30
10.8	-37	18	24	-34
11.8	-45	0	3	-43
12.4	-51	7	10	-47
12.5	-52	14	22	-49
12.7	-54	17	24	-50
12.8	-55	19	24	-52

999 DENOTES MISSING DATA

RMSS RADIOSONDE TEST FLIGHT #22

ALT-KM	CH#1	CH#2	CH#3	CH#4
0.0	21	24	90	26
1.0	16	20	73	21
2.0	12	15	90	17
3.0	10	13	14	15
4.0	5	7	14	10
5.0	0	2	15	4
6.0	-6	-3	13	1
7.0	-12	-9	11	-6
8.0	-19	-16	11	-14
9.0	-26	-23	13	-21
10.1	-33	-30	80	-28
11.0	-38	-35	42	-33
12.0	-44	-42	39	-40
13.0	-52	-49	40	-47
14.0	-59	-57	35	-55
15.2	-65	-62	37	-61
16.3	-72	-69	37	-68
17.4	-80	-77	37	-75
18.4	-86	-83	37	-82
19.8	-84	-81	37	-80
20.4	-78	-75	37	-74
21.3	-68	-65	37	-65
22.4	-69	-66	36	-65
23.4	-63	-62	36	-60
24.5	-60	-58	34	-57
25.5	-53	-50	32	-51
26.7	-49	-47	28	-46
27.8	-51	-48	26	-47
29.0	-51	-49	25	-48
30.1	-49	-46	24	-47
31.2	-45	-43	25	-42
32.3	-45	-42	24	-42
33.4	-43	-41	14	-41
34.5	-41	-40	24	-39
35.6	-42	-41	27	-40
36.7	-36	-36	27	-34
37.8	-30	-32	26	-29

RMSS RADIOSONDE TEST FLIGHT #21

ALT-KM	CH#1	CH#2	CH#3	CH#4
0.0	92	26	91	25
1.0	95	20	93	20
2.0	14	17	13	16
3.0	10	14	10	13
4.0	10	8	10	8
5.0	14	2	15	2
6.0	50	-3	48	-3
7.0	9	-9	9	-2
8.0	9	-16	9	-16
9.0	9	-23	9	-23
10.0	10	-32	10	-32
11.0	19	-38	18	-38
12.0	23	-48	23	-48
13.0	31	-56	32	-56

DISTRIBUTION LIST

Dr. Frank D. Eaton
Geophysical Institute
University of Alaska
Fairbanks, AK 99701

Commander
US Army Aviation Center
ATTN: ATZQ-D-MA
Fort Rucker, AL 36362

Chief, Atmospheric Sciences Div
Code ES-81
NASA
Marshall Space Flight Center,
AL 35812

Commander
US Army Missile R&D Command
ATTN: DRDMI-CGA (B. W. Fowler)
Redstone Arsenal, AL 35809

Redstone Scientific Information Center
ATTN: DRDMI-TBD
US Army Missile R&D Command
Redstone Arsenal, AL 35809

Commander
US Army Missile R&D Command
ATTN: DRDMI-TEM (R. Haraway)
Redstone Arsenal, AL 35809

Commander
US Army Missile R&D Command
ATTN: DRDMI-TRA (Dr. Essenwanger)
Redstone Arsenal, AL 35809

Commander
HQ, Fort Huachuca
ATTN: Tech Ref Div
Fort Huachuca, AZ 85613

Commander
US Army Intelligence Center & School
ATTN: ATSI-CD-MD
Fort Huachuca, AZ 85613

Commander
US Army Yuma Proving Ground
ATTN: Technical Library
Bldg 2100
Yuma, AZ 85364

Naval Weapons Center (Code 3173)
ATTN: Dr. A. Shlanta
China Lake, CA 93555

Sylvania Elec Sys Western Div
ATTN: Technical Reports Library
PO Box 205
Mountain View, CA 94040

Geophysics Officer
PMTC Code 3250
Pacific Missile Test Center
Point Mugu, CA 93042

Commander
Naval Ocean Systems Center (Code 4473)
ATTN: Technical Library
San Diego, CA 92152

Meteorologist in Charge
Kwajalein Missile Range
PO Box 67
APO San Francisco, 96555

Director
NOAA/ERL/APCL R31
RB3-Room 567
Boulder, CO 80302

Library-R-51-Tech Reports
NOAA/ERL
320 S. Broadway
Boulder, CO 80302

National Center for Atmos Research
NCAR Library
PO Box 3000
Boulder, CO 80307

B. Girardo
Bureau of Reclamation
E&R Center, Code 1220
Denver Federal Center, Bldg 67
Denver, CO 80225

National Weather Service
National Meteorological Center
W321, WWB, Room 201
ATTN: Mr. Quiroz
Washington, DC 20233

Mil Assistant for Atmos Sciences
Ofc of the Undersecretary of Defense
for Rsch & Engr/E&LS - Room 3D129
The Pentagon
Washington, DC 20301

Defense Communications Agency
Technical Library Center
Code 205
Washington, DC 20305

Director
Defense Nuclear Agency
ATTN: Technical Library
Washington, DC 20305

HQDA (DAEN-RDM/Dr. de Percin)
Washington, DC 20314

Director
Naval Research Laboratory
Code 5530
Washington, DC 20375

Commanding Officer
Naval Research Laboratory
Code 2627
Washington, DC 20375

Dr. J. M. MacCallum
Naval Research Laboratory
Code 1409
Washington, DC 20375

The Library of Congress
ATTN: Exchange & Gift Div
Washington, DC 20540
2

Head, Atmos Rsch Section
Div Atmospheric Science
National Science Foundation
1800 G. Street, NW
Washington, DC 20550

CPT Hugh Albers, Exec Sec
Interdept Committee on Atmos Science
National Science Foundation
Washington, DC 20550

Director, Systems R&D Service
Federal Aviation Administration
ATTN: ARD-54
2100 Second Street, SW
Washington, DC 20590

ADTC/DLODL
Eglin AFB, FL 32542

Naval Training Equipment Center
ATTN: Technical Library
Orlando, FL 32813

Det 11, 2WS/OI
ATTN: Maj Orondorff
Patrick AFB, FL 32925

USAFETAC/CB
Scott AFB, IL 62225

HQ, ESD/TOSI/S-22
Hanscom AFB, MA 01731

Air Force Geophysics Laboratory
ATTN: LCB (A. S. Carten, Jr.)
Hanscom AFB, MA 01731

Air Force Geophysics Laboratory
ATTN: LYD
Hanscom AFB, MA 01731

Meteorology Division
AFGL/LY
Hanscom AFB, MA 01731

US Army Liaison Office
MIT-Lincoln Lab, Library A-082
PO Box 73
Lexington, MA 02173

Director
US Army Ballistic Rsch Lab
ATTN: DRDAR-BLB (Dr. G. E. Keller)
Aberdeen Proving Ground, MD 21005

Commander
US Army Ballistic Rsch Lab
ATTN: DRDAR-BLP
Aberdeen Proving Ground, MD 21005

Director
US Army Armament R&D Command
Chemical Systems Laboratory
ATTN: DRDAR-CLJ-I
Aberdeen Proving Ground, MD 21010

Chief CB Detection & Alarms Div
Chemical Systems Laboratory
ATTN: DRDAR-CLC-CR (H. Tannenbaum)
Aberdeen Proving Ground, MD 21010

Commander
Harry Diamond Laboratories
ATTN: DELHD-CO
2800 Powder Mill Road
Adelphi, MD 20783

Commander
ERADCOM
ATTN: DRDEL-AP
2800 Powder Mill Road
Adelphi, MD 20783
2

Commander
ERADCOM
ATTN: DRDEL-CG/DRDEL-DC/DRDEL-CS
2800 Powder Mill Road
Adelphi, MD 20783

Commander
ERADCOM
ATTN: DRDEL-CT
2800 Powder Mill Road
Adelphi, MD 20783

Commander
ERADCOM
ATTN: DRDEL-EA
2800 Powder Mill Road
Adelphi, MD 20783

Commander
ERADCOM
ATTN: DRDEL-PA/DRDEL-ILS/DRDEL-E
2800 Powder Mill Road
Adelphi, MD 20783

Commander
ERADCOM
ATTN: DRDEL-PAO (S. Kimmel)
2800 Powder Mill Road
Adelphi, MD 20783

Chief
Intelligence Materiel Dev & Support Ofc
ATTN: DELEW-WL-I
Bldg 4554
Fort George G. Meade, MD 20755

Acquisitions Section, IRDB-D823
Library & Info Service Div, NOAA
6009 Executive Blvd
Rockville, MD 20852

Naval Surface Weapons Center
White Oak Library
Silver Spring, MD 20910

The Environmental Research
Institute of MI
ATTN: IRIA Library
PO Box 8618
Ann Arbor, MI 48107

Mr. William A. Main
USDA Forest Service
1407 S. Harrison Road
East Lansing, MI 48823

Dr. A. D. Belmont
Research Division
PO Box 1249
Control Data Corp
Minneapolis, MN 55440

Director
Naval Oceanography & Meteorology
NSTL Station
Bay St Louis, MS 39529

Director
US Army Engr Waterways Experiment Sta
ATTN: Library
PO Box 631
Vicksburg, MS 39180

Environmental Protection Agency
Meteorology Laboratory
Research Triangle Park, NC 27711

US Army Research Office
ATTN: DRXRO-PP
PO Box 12211
Research Triangle Park, NC 27709

Commanding Officer
US Army Armament R&D Command
ATTN: DRDAR-TSS Bldg 59
Dover, NJ 07801

Commander
HQ, US Army Avionics R&D Activity
ATTN: DAVAA-O
Fort Monmouth, NJ 07703

Commander/Director
US Army Combat Surveillance & Target
Acquisition Laboratory
ATTN: DELCS-D
Fort Monmouth, NJ 07703

Commander
US Army Electronics R&D Command
ATTN: DELCS-S
Fort Monmouth, NJ 07703

US Army Materiel Systems
Analysis Activity
ATTN: DRXSY-MP
Aberdeen Proving Ground, MD 21005

Director
US Army Electronics Technology &
Devices Laboratory
ATTN: DELET-D
Fort Monmouth, NJ 07703

Commander
US Army Electronic Warfare Laboratory
ATTN: DELEW-D
Fort Monmouth, NJ 07703

Commander
US Army Night Vision &
Electro-Optics Laboratory
ATTN: DELNV-L (Dr. Rudolf Buser)
Fort Monmouth, NJ 07703

Commander
ERADCOM Technical Support Activity
ATTN: DELSD-L
Fort Monmouth, NJ 07703

Project Manager, FIREFINDER
ATTN: DRCPM-FF
Fort Monmouth, NJ 07703

Project Manager, REMBASS
ATTN: DRCPM-RBS
Fort Monmouth, NJ 07703

Commander
US Army Satellite Comm Agency
ATTN: DRCPM-SC-3
Fort Monmouth, NJ 07703

Commander
ERADCOM Scientific Advisor
ATTN: DRDEL-SA
Fort Monmouth, NJ 07703

6585 TG/WE
Holloman AFB, NM 88330

AFWL/WE
Kirtland, AFB, NM 87117

AFWL/Technical Library (SUL)
Kirtland AFB, NM 87117

Commander
US Army Test & Evaluation Command
ATTN: STEWS-AD-L
White Sands Missile Range, NM 88002

Rome Air Development Center
ATTN: Documents Library
TSLD (Bette Smith)
Griffiss AFB, NY 13441

Commander
US Army Tropic Test Center
ATTN: STETC-TD (Info Center)
APO New York 09827

Commandant
US Army Field Artillery School
ATTN: ATSF-CD-R (Mr. Farmer)
Fort Sill, OK 73503

Commandant
US Army Field Artillery School
ATTN: ATSF-CF-R
Fort Sill, OK 73503

Director CFD
US Army Field Artillery School
ATTN: Met Division
Fort Sill, OK 73503

Commandant
US Army Field Artillery School
ATTN: Morris Swett Library
Fort Sill, OK 73503

Commander
US Army Dugway Proving Ground
ATTN: MT-DA-L
Dugway, UT 84022

William Peterson
Research Associates
Utah State University, UNC 48
Logan, UT 84322

Inge Dirmhirn, Professor
Utah State University, UNC 48
Logan, UT 84322

Defense Documentation Center
ATTN: DDC-TCA
Cameron Station, Bldg 5
Alexandria, VA 22314
12

Commanding Officer
US Army Foreign Sci & Tech Center
ATTN: DRXST-IS1
220 7th Street, NE
Charlottesville, VA 22901

Naval Surface Weapons Center
Code G65
Dahlgren, VA 22448

Commander
US Army Night Vision
& Electro-Optics Lab
ATTN: DELNV-D
Fort Belvoir, VA 22060

Commander and Director
US Army Engineer Topographic Lab
ETL-TD-MB
Fort Belvoir, VA 22060

Director
Applied Technology Lab
DAVDL-EU-TSD
ATTN: Technical Library
Fort Eustis, VA 23604

Department of the Air Force
OL-C, 5WW
Fort Monroe, VA 23651

Department of the Air Force
5WW/DN
Langley AFB, VA 23665

Director
Development Center MCDEC
ATTN: Firepower Division
Quantico, VA 22134

US Army Nuclear & Chemical Agency
ATTN: MONA-WE
Springfield, VA 22150

Director
US Army Signals Warfare Laboratory
ATTN: DELSW-OS (Dr. R. Burkhardt)
Vint Hill Farms Station
Warrenton, VA 22186

Commander
US Army Cold Regions Test Center
ATTN: STECR-OP-PM
APO Seattle, 98733

Commander
US Army Dugway Proving Ground
ATTN: STEDP-MT-DA-M (Mr. Paul Carlson)
Dugway, UT 84022

Commander
TRASANA
ATTN: DELAS-ATAA-PL
(Dolores Anguiano)
White Sands Missile Range, NM 88002

ATMOSPHERIC SCIENCES RESEARCH PAPERS

1. Lindberg, J.D., "An Improvement to a Method for Measuring the Absorption Coefficient of Atmospheric Dust and other Strongly Absorbing Powders," ECOM-5565, July 1975.
2. Avara, Elton P., "Mesoscale Wind Shears Derived from Thermal Winds," ECOM-5566, July 1975.
3. Gomez, Richard B., and Joseph H. Pierluissi, "Incomplete Gamma Function Approximation for King's Strong-Line Transmittance Model," ECOM-5567, July 1975.
4. Blanco, A.J., and B.F. Engebos, "Ballistic Wind Weighting Functions for Tank Projectiles," ECOM-5568, August 1975.
5. Taylor, Fredrick J., Jack Smith, and Thomas H. Pries, "Crosswind Measurements through Pattern Recognition Techniques," ECOM-5569, July 1975.
6. Walters, D.L., "Crosswind Weighting Functions for Direct-Fire Projectiles," ECOM-5570, August 1975.
7. Duncan, Louis D., "An Improved Algorithm for the Iterated Minimal Information Solution for Remote Sounding of Temperature," ECOM-5571, August 1975.
8. Robbiani, Raymond L., "Tactical Field Demonstration of Mobile Weather Radar Set AN/TPS-41 at Fort Rucker, Alabama," ECOM-5572, August 1975.
9. Miers, B., G. Blackman, D. Langer, and N. Lorimier, "Analysis of SMS/GOES Film Data," ECOM-5573, September 1975.
10. Manquero, Carlos, Louis Duncan, and Rufus Bruce, "An Indication from Satellite Measurements of Atmospheric CO₂ Variability," ECOM-5574, September 1975.
11. Petracca, Carmine, and James D. Lindberg, "Installation and Operation of an Atmospheric Particulate Collector," ECOM-5575, September 1975.
12. Avara, Elton P., and George Alexander, "Empirical Investigation of Three Iterative Methods for Inverting the Radiative Transfer Equation," ECOM-5576, October 1975.
13. Alexander, George D., "A Digital Data Acquisition Interface for the SMS Direct Readout Ground Station - Concept and Preliminary Design," ECOM-5577, October 1975.
14. Cantor, Israel, "Enhancement of Point Source Thermal Radiation Under Clouds in a Nonattenuating Medium," ECOM-5578, October 1975.
15. Norton, Colburn, and Glenn Hoidale, "The Diurnal Variation of Mixing Height by Month over White Sands Missile Range, N.M.," ECOM-5579, November 1975.
16. Avara, Elton P., "On the Spectrum Analysis of Binary Data," ECOM-5580, November 1975.
17. Taylor, Fredrick J., Thomas H. Pries, and Chao-Huan Huang, "Optimal Wind Velocity Estimation," ECOM-5581, December 1975.
18. Avara, Elton P., "Some Effects of Autocorrelated and Cross-Correlated Noise on the Analysis of Variance," ECOM-5582, December 1975.
19. Gillespie, Patti S., R.L. Armstrong, and Kenneth O. White, "The Spectral Characteristics and Atmospheric CO₂ Absorption of the Ho³⁺ YLF Laser at 2.05 μ m," ECOM-5583, December 1975.
20. Novlan, David J. "An Empirical Method of Forecasting Thunderstorms for the White Sands Missile Range," ECOM-5584, February 1976.
21. Avara, Elton P., "Randomization Effects in Hypothesis Testing with Autocorrelated Noise," ECOM-5585, February 1976.
22. Watkins, Wendell R., "Improvements in Long Path Absorption Cell Measurement," ECOM-5586, March 1976.
23. Thomas, Joe, George D. Alexander, and Marvin Dubbin, "SATTEL - An Army Dedicated Meteorological Telemetry System," ECOM-5587, March 1976.
24. Kennedy, Bruce W., and Delbert Bynum, "Army User Test Program for the RDT&E-XM-75 Meteorological Rocket," ECOM-5588, April 1976.

25. Barnett, Kenneth M., "A Description of the Artillery Meteorological Comparisons at White Sands Missile Range, October 1974 - December 1974 ('PASS' - Prototype Artillery [Meteorological] Subsystem)," ECOM-5589, April 1976.
26. Miller, Walter B., "Preliminary Analysis of Fall-of-Shot From Project 'PASS'," ECOM-5590, April 1976.
27. Avara, Elton P., "Error Analysis of Minimum Information and Smith's Direct Methods for Inverting the Radiative Transfer Equation," ECOM-5591, April 1976.
28. Yee, Young P., James D. Horn, and George Alexander, "Synoptic Thermal Wind Calculations from Radiosonde Observations Over the Southwestern United States," ECOM-5592, May 1976.
29. Duncan, Louis D., and Mary Ann Seagraves, "Applications of Empirical Corrections to NOAA-4 VTPR Observations," ECOM-5593, May 1976.
30. Miers, Bruce T., and Steve Weaver, "Applications of Meteorological Satellite Data to Weather Sensitive Army Operations," ECOM-5594, May 1976.
31. Sharenow, Moses, "Redesign and Improvement of Balloon ML-566," ECOM-5595, June, 1976.
32. Hansen, Frank V., "The Depth of the Surface Boundary Layer," ECOM-5596, June 1976.
33. Pinnick, R.G., and E.B. Stenmark, "Response Calculations for a Commercial Light-Scattering Aerosol Counter," ECOM-5597, July 1976.
34. Mason, J., and G.B. Hoidale, "Visibility as an Estimator of Infrared Transmittance," ECOM-5598, July 1976.
35. Bruce, Rufus E., Louis D. Duncan, and Joseph H. Pierluissi, "Experimental Study of the Relationship Between Radiosonde Temperatures and Radiometric-Area Temperatures," ECOM-5599, August 1976.
36. Duncan, Louis D., "Stratospheric Wind Shear Computed from Satellite Thermal Sounder Measurements," ECOM-5800, September 1976.
37. Taylor, F., P. Mohan, P. Joseph and T. Pries, "An All Digital Automated Wind Measurement System," ECOM-5801, September 1976.
38. Bruce, Charles, "Development of Spectrophones for CW and Pulsed Radiation Sources," ECOM-5802, September 1976.
39. Duncan, Louis D., and Mary Ann Seagraves, "Another Method for Estimating Clear Column Radiances," ECOM-5803, October 1976.
40. Blanco, Abel J., and Larry E. Taylor, "Artillery Meteorological Analysis of Project Pass," ECOM-5804, October 1976.
41. Miller, Walter, and Bernard Engebos, "A Mathematical Structure for Refinement of Sound Ranging Estimates," ECOM-5805, November, 1976.
42. Gillespie, James B., and James D. Lindberg, "A Method to Obtain Diffuse Reflectance Measurements from 1.0 to 3.0 μm Using a Cary 171 Spectrophotometer," ECOM-5806, November 1976.
43. Rubio, Roberto, and Robert O. Olsen, "A Study of the Effects of Temperature Variations on Radio Wave Absorption," ECOM-5807, November 1976.
44. Ballard, Harold N., "Temperature Measurements in the Stratosphere from Balloon-Borne Instrument Platforms, 1968-1975," ECOM-5808, December 1976.
45. Monahan, H.H., "An Approach to the Short-Range Prediction of Early Morning Radiation Fog," ECOM-5809, January 1977.
46. Engebos, Bernard Francis, "Introduction to Multiple State Multiple Action Decision Theory and Its Relation to Mixing Structures," ECOM-5810, January 1977.
47. Low, Richard D.H., "Effects of Cloud Particles on Remote Sensing from Space in the 10-Micrometer Infrared Region," ECOM-5811, January 1977.
48. Bonner, Robert S., and R. Newton, "Application of the AN/GVS-5 Laser Rangefinder to Cloud Base Height Measurements," ECOM-5812, February 1977.
49. Rubio, Roberto, "Lidar Detection of Subvisible Reentry Vehicle Erosive Atmospheric Material," ECOM-5813, March 1977.
50. Low, Richard D.H., and J.D. Horn, "Mesoscale Determination of Cloud-Top Height: Problems and Solutions," ECOM-5814, March 1977.

51. Duncan, Louis D., and Mary Ann Seagraves, "Evaluation of the NOAA-4 VTPR Thermal Winds for Nuclear Fallout Predictions," ECOM-5815, March 1977.
52. Randhawa, Jagir S., M. Izquierdo, Carlos McDonald and Zvi Salpeter, "Stratospheric Ozone Density as Measured by a Chemiluminescent Sensor During the Stratcom VI-A Flight," ECOM-5816, April 1977.
53. Rubio, Roberto, and Mike Izquierdo, "Measurements of Net Atmospheric Irradiance in the 0.7- to 2.8-Micrometer Infrared Region," ECOM-5817, May 1977.
54. Ballard, Harold N., Jose M. Serna, and Frank P. Hudson Consultant for Chemical Kinetics, "Calculation of Selected Atmospheric Composition Parameters for the Mid-Latitude, September Stratosphere," ECOM-5818, May 1977.
55. Mitchell, J.D., R.S. Sagar, and R.O. Olsen, "Positive Ions in the Middle Atmosphere During Sunrise Conditions," ECOM-5819, May 1977.
56. White, Kenneth O., Wendell R. Watkins, Stuart A. Schleusener, and Ronald L. Johnson, "Solid-State Laser Wavelength Identification Using a Reference Absorber," ECOM-5820, June 1977.
57. Watkins, Wendell R., and Richard G. Dixon, "Automation of Long-Path Absorption Cell Measurements," ECOM-5821, June 1977.
58. Taylor, S.E., J.M. Davis, and J.B. Mason, "Analysis of Observed Soil Skin Moisture Effects on Reflectance," ECOM-5822, June 1977.
59. Duncan, Louis D. and Mary Ann Seagraves, "Fallout Predictions Computed from Satellite Derived Winds," ECOM-5823, June 1977.
60. Snider, D.E., D.G. Murcay, F.H. Murcay, and W.J. Williams, "Investigation of High-Altitude Enhanced Infrared Background Emissions" (U), SECRET, ECOM-5824, June 1977.
61. Dubbin, Marvin H. and Dennis Hall, "Synchronous Meteorological Satellite Direct Readout Ground System Digital Video Electronics," ECOM-5825, June 1977.
62. Miller, W., and B. Engebos, "A Preliminary Analysis of Two Sound Ranging Algorithms," ECOM-5826, July 1977.
63. Kennedy, Bruce W., and James K. Luers, "Ballistic Sphere Techniques for Measuring Atmospheric Parameters," ECOM-5827, July 1977.
64. Duncan, Louis D., "Zenith Angle Variation of Satellite Thermal Sounder Measurements," ECOM-5828, August 1977.
65. Hansen, Frank V., "The Critical Richardson Number," ECOM-5829, September 1977.
66. Ballard, Harold N., and Frank P. Hudson (Compilers), "Stratospheric Composition Balloon-Borne Experiment," ECOM-5830, October 1977.
67. Barr, William C., and Arnold C. Peterson, "Wind Measuring Accuracy Test of Meteorological Systems," ECOM-5831, November 1977.
68. Ethridge, G.A. and F.V. Hansen, "Atmospheric Diffusion: Similarity Theory and Empirical Derivations for Use in Boundary Layer Diffusion Problems," ECOM-5832, November 1977.
69. Low, Richard D.H., "The Internal Cloud Radiation Field and a Technique for Determining Cloud Blackness," ECOM-5833, December 1977.
70. Watkins, Wendell R., Kenneth O. White, Charles W. Bruce, Donald L. Walters, and James D. Lindberg, "Measurements Required for Prediction of High Energy Laser Transmission," ECOM-5834, December 1977.
71. Rubio, Robert, "Investigation of Abrupt Decreases in Atmospherically Backscattered Laser Energy," ECOM-5835, December 1977.
72. Monahan, H.H. and R.M. Cionco, "An Interpretative Review of Existing Capabilities for Measuring and Forecasting Selected Weather Variables (Emphasizing Remote Means)," ASL-TR-0001, January 1978.
73. Heaps, Melvin G., "The 1979 Solar Eclipse and Validation of D-Region Models," ASL-TR-0002, March 1978.

74. Jennings, S.G., and J.B. Gillespie, "M.I.E. Theory Sensitivity Studies - The Effects of Aerosol Complex Refractive Index and Size Distribution Variations on Extinction and Absorption Coefficients Part II: Analysis of the Computational Results," ASL-TR-0003, March 1978.
75. White, Kenneth O. et al, "Water Vapor Continuum Absorption in the 3.5 μ m to 4.0 μ m Region," ASL-TR-0004, March 1978.
76. Olsen, Robert O., and Bruce W. Kennedy, "ABRES Pretest Atmospheric Measurements," ASL-TR-0005, April 1978.
77. Ballard, Harold N., Jose M. Serna, and Frank P. Hudson, "Calculation of Atmospheric Composition in the High Latitude September Stratosphere," ASL-TR-0006, May 1978.
78. Watkins, Wendell R. et al, "Water Vapor Absorption Coefficients at HF Laser Wavelengths," ASL-TR-0007, May 1978.
79. Hansen, Frank V., "The Growth and Prediction of Nocturnal Inversions," ASL-TR-0008, May 1978.
80. Samuel, Christine, Charles Bruce, and Ralph Brewer, "Spectrophone Analysis of Gas Samples Obtained at Field Site," ASL-TR-0009, June 1978.
81. Pinnick, R.G. et al., "Vertical Structure in Atmospheric Fog and Haze and its Effects on IR Extinction," ASL-TR-0010, July 1978.
82. Low, Richard D.H., Louis D. Duncan, and Richard B. Gomez, "The Microphysical Basis of Fog Optical Characterization," ASL-TR-0011, August 1978.
83. Heaps, Melvin G., "The Effect of a Solar Proton Event on the Minor Neutral Constituents of the Summer Polar Mesosphere," ASL-TR-0012, August 1978.
84. Mason, James B., "Light Attenuation in Falling Snow," ASL-TR-0013, August 1978.
85. Blanco, Abel J., "Long-Range Artillery Sound Ranging: "PASS" Meteorological Application," ASL-TR-0014, September 1978.
86. Heaps, M.G., and F.E. Niles, "Modeling the Ion Chemistry of the D-Region: A case Study Based Upon the 1966 Total Solar Eclipse," ASL-TR-0015, September 1978.
87. Jennings, S.G., and R.G. Pinnick, "Effects of Particulate Complex Refractive Index and Particle Size Distribution Variations on Atmospheric Extinction and Absorption for Visible Through Middle-Infrared Wavelengths," ASL-TR-0016, September 1978.
88. Watkins, Wendell R., Kenneth O. White, Lanny R. Bower, and Brian Z. Sojka, "Pressure Dependence of the Water Vapor Continuum Absorption in the 3.5- to 4.0-Micrometer Region," ASL-TR-0017, September 1978.
89. Miller, W.B., and B.F. Engebos, "Behavior of Four Sound Ranging Techniques in an Idealized Physical Environment," ASL-TR-0018, September 1978.
90. Gomez, Richard G., "Effectiveness Studies of the CBU-88/B Bomb, Cluster, Smoke Weapon" (U), CONFIDENTIAL ASL-TR-0019, September 1978.
91. Miller, August, Richard C. Shirkey, and Mary Ann Seagraves, "Calculation of Thermal Emission from Aerosols Using the Doubling Technique," ASL-TR-0020, November, 1978.
92. Lindberg, James D. et al., "Measured Effects of Battlefield Dust and Smoke on Visible, Infrared, and Millimeter Wavelengths Propagation: A Preliminary Report on Dusty Infrared Test-I (DIRT-I)," ASL-TR-0021, January 1979.
93. Kennedy, Bruce W., Arthur Kinghorn, and B.R. Hixon, "Engineering Flight Tests of Range Meteorological Sounding System Radiosonde," ASL-TR-0022, February 1979.